ISSN 2075-8545 (online)

Nanotechnologies in construction
Нанотехнологии в строительстве

2026; 18 (3):
317–340

Nanobuild.ru

MANUFACTURING TECHNOLOGY FOR BUILDING MATERIALS AND PRODUCTS

Original article
https://doi.org/10.15828/2075-8545-2026-18-3-317-340

Effects of various types of fiber reinforcement on the physico-mechanical characteristics and hydrophobic properties of high-strength concrete for hydraulic structures

Manizha Paktin[1], Alibek M. Imanov[2]*, Karlygash I. Ilyassova[1]*, Orazaly D. Seitkazinov[1, 3], Manat T. Nogaibekova[4], Zhangazy N. Moldamuratov[1, 3]

[1] International Educational Corporation, 050043, Almaty, 28 K. Ryskulbekov Street, Kazakhstan
[2] Abylkas Saginov Karaganda Technical University, 100027, Karaganda, 56 N. Nazarbayev Avenue, Kazakhstan
[3] Kazakh Leading Academy of Architecture and Civil Engineering, 050043, Almaty, 29 Toraigyrov Street, Kazakhstan
[4] Kazakh National University of Water Management and Irrigation, 080003, Taraz, 28 Satpayev Street, Kazakhstan

* Corresponding authors: e-mail: alibek.imanov@mail.ru, k.iliasova@kazgasa.kz

ABSTRACT

Introduction. One of the most effective ways to improve the performance characteristics of concrete is dispersed reinforcement with various types of fibers. This study investigates the influence of steel, basalt, polypropylene, and glass fibers on the physico-mechanical and hydrophysical properties of concrete. **Materials and Methods.** Concrete without fiber reinforcement was used as the reference mixture (REF). The reinforced mixtures included steel fiber (SF), basalt fiber (BF), polypropylene fiber (PPF), and glass fiber (GF). Tests were carried out to determine compressive strength, flexural strength, and splitting tensile strength. In addition, the modulus of elasticity, crack width, water absorption, capillary water absorption, water impermeability, sulfate resistance, frost resistance, and resistance to wetting-drying cycles were evaluated. **Results and Discussion.** It was established that the incorporation of fibers contributes to an increase in the strength and durability of concrete. The highest compressive strength at the age of 28 days was obtained for the SF mixture, reaching 79.6 MPa, which is 16.4% higher than that of the reference mixture REF (68.4 MPa). For BF, this value was 76.8 MPa (+12.3%), for GF 74.5 MPa (+8.9%), and for PPF 72.9 MPa (+6.6%). Flexural strength increased from 7.8 MPa for REF to 11.2 MPa for SF (+43.6%) and 10.4 MPa for BF (+33.3%). The width of the main crack decreased from 0.95 mm for REF to 0.42 mm for SF and 0.48 mm for BF. Water absorption decreased from 4.82% for REF to 3.41% for SF and 3.56% for BF, while the capillary absorption coefficient decreased from 0.184 to 0.121 kg/(m^2•h^0.5) for SF. The water impermeability grade increased from W10 to W14. Durability tests showed that the mass loss after 180 days of sulfate exposure decreased from 2.8% for REF to 1.2% for SF and 1.4% for BF, while the strength retention coefficient increased to 90.3% and 89.4%, respectively. After 300 freeze-thaw cycles, the mass loss amounted to 1.8% for SF and 2.1% for BF, compared to 4.6% for REF. **Conclusion.** Based on the overall physico-mechanical and hydrophysical performance, steel and basalt fibers were found to be the most effective types of dispersed reinforcement. Their use provides an increase in compressive strength of up to 16.4%, an increase in flexural strength of up to 43.6%, a reduction in water absorption of up to 29.3%, a more than twofold decrease in crack width, and a significant improvement in the resistance of concrete to aggressive environmental factors.

KEYWORDS: fiber-reinforced concrete; hydrophobic concrete; micro- and nanostructure of concrete; sustainable construction

SOURCES OF FUNDING FOR THE SCIENTIFIC WORK THAT RESULTED IN THE PUBLICATION: The research was carried out with the financial support of the Committee of Science of the Ministry of Science and Higher Education of the Republic of Kazakhstan within the framework of the scientific project No. AP23487624.

FOR CITATION:
Paktin M., Imanov A.M., Ilyassova K.I., Seitkazinov O.D., Nogaibekova M.T., Moldamuratov Zh.N. Effects of various types of fiber reinforcement on the physico-mechanical characteristics and hydrophobic properties of high-strength concrete for hydraulic structures. *Nanotechnologies in Construction.* 2026;18(3):317–340. https://doi.org/10.15828/2075-8545-2026-18-3-317-340. – EDN: TWRUUP.

ISSN 2075-8545 (online)

Nanotechnologies in construction
Нанотехнологии в строительстве

2026; 18 (3):
317–340

Nanobuild.ru

MANUFACTURING TECHNOLOGY FOR BUILDING MATERIALS AND PRODUCTS

Влияние различных типов фибрового армирования на физико-механические характеристики и гидрофобные свойства высокопрочных гидротехнических бетонов

Манижа Пактин[1], Алибек Маратович Иманов[2]*, Карлыгаш Идрисовна Ильясова[1]*, Оразалы Дауткалиевич Сейтказинов[1, 3], Манат Тузельбековна Ногайбекова[4], Жангазы Нуржанович Молдамуратов[1, 3]

[1] Международная образовательная корпорация, 050043, Алматы, ул. К. Рыскулбекова, 28, Казахстан

[2] Карагандинский технический университет имени Абылкаса Сагинова, 100027, Караганда, пр. Н. Назарбаева, 56, Казахстан

[3] Казахская головная архитектурно-строительная академия, 050043, Алматы, ул. Торайгырова, 29, Казахстан

[4] Казахский национальный университет водного хозяйства и ирригации, 080003, Тараз, ул. Сатпаева, 28, Казахстан

* Авторы, ответственные за переписку: e-mail: alibek.imanov@mail.ru, k.iliasova@kazgasa.kz

АННОТАЦИЯ

Введение. Одним из эффективных способов повышения эксплуатационных характеристик бетона является дисперсное армирование различными видами фибры. В данной работе исследовано влияние стальной, базальтовой, полипропиленовой и стеклянной фибры на физико-механические и гидрофизические свойства бетона. **Методы и материалы.** В качестве контрольного состава использован бетон без фибры (REF). Армированные составы включали стальную (SF), базальтовую (BF), полипропиленовую (PPF) и стеклянную (GF) фибру. Выполнены испытания на прочность при сжатии, изгибе и раскалывании, определены модуль упругости, ширина раскрытия трещин, показатели водопоглощения, капиллярного всасывания, водонепроницаемости, сульфатной стойкости, морозостойкости и стойкости к циклам увлажнения-высыхания. **Результаты и обсуждение.** Установлено, что применение фибры способствует повышению прочности и долговечности бетона. Наибольшая прочность при сжатии в возрасте 28 сут. получена у состава SF – 79,6 МПа, что на 16,4% выше контрольного состава REF (68,4 МПа). Для BF данный показатель составил 76,8 МПа (+12,3%), для GF – 74.5 МПа (+8,9%), для PPF – 72,9 МПа (+6,6%). Прочность при изгибе возросла с 7,8 МПа у REF до 11,2 МПа у SF (+43,6%) и 10,4 МПа у BF (+33,3%). Ширина раскрытия основной трещины уменьшилась с 0,95 мм у REF до 0,42 мм у SF и 0,48 мм у BF. Водопоглощение снизилось с 4,82% у REF до 3,41% у SF и 3,56% у BF, а коэффициент капиллярного всасывания уменьшился с 0,184 до 0,121 кг/(м^2•ч0,5) для SF. Марка по водонепроницаемости повысилась с W10 до W14. Испытания на долговечность показали, что потеря массы после 180 сут. сульфатного воздействия уменьшилась с 2,8% у REF до 1,2% у SF и 1,4% у BF, а коэффициент сохранения прочности повысился до 90,3% и 89,4% соответственно. После 300 циклов замораживания-оттаивания потеря массы составила 1,8% для SF и 2,1% для BF против 4,6% у REF. **Заключение.** По совокупности физико-механических и гидрофизических показателей наиболее эффективными видами дисперсного армирования являются стальная и базальтовая фибра. Их применение обеспечивает повышение прочности при сжатии до 16,4%, увеличение прочности при изгибе до 43,6%, снижение водопоглощения до 29,3%, уменьшение ширины раскрытия трещин более чем в 2 раза и существенное повышение стойкости бетона к воздействию агрессивных факторов среды.

КЛЮЧЕВЫЕ СЛОВА: фибробетон; гидрофобный бетон; микро и наноструктура бетона; устойчивое строительство

ИСТОЧНИКИ ФИНАНСИРОВАНИЯ НАУЧНОЙ РАБОТЫ, РЕЗУЛЬТАТОМ КОТОРОЙ СТАЛА ПУБЛИКАЦИЯ: Исследование выполнено при финансовой поддержке Комитета науки Министерства науки и высшего образования Республики Казахстан в рамках научного проекта № AP23487624.

ДЛЯ ЦИТИРОВАНИЯ:
Пактин М., Иманов А.М., Ильясова К.И., Сейтказинов О.Д., Ногайбекова М.Т., Молдамуратов Ж.Н. Влияние различных типов фибрового армирования на физико-механические характеристики и гидрофобные свойства высокопрочных гидротехнических бетонов. *Нанотехнологии в строительстве.* 2026;18(3):317–340. https://doi.org/10.15828/2075- 8545-2026-18-3-317-340. – EDN: TWRUUP.

INTRODUCTION

High-strength concrete is increasingly being used in the construction and rehabilitation of hydraulic structures due to its high load-bearing capacity, low permeability, and enhanced durability. The application of such materials is particularly relevant for irrigation canal linings operating under conditions of постоянного moisture exposure, alternating wetting and drying, cyclic freezing and thawing, abrasive action of flowing water, as well as

ISSN 2075-8545 (online)
Nanotechnologies in construction
Нанотехнологии в строительстве
2026; 18 (3): 317–340
Nanobuild.ru

chemical attack caused by sulfates and salts present in soils and irrigation water [1, 2].

This issue is especially important for the southern regions of Kazakhstan. The largest share of water consumption in the country is associated with agriculture, with more than 60–70% of total water resources being used for irrigation purposes. In 2024, approximately 10.9 km³ of irrigation water was supplied to southern Kazakhstan, accounting for 97% of the total volume of water allocated for irrigation needs nationwide [1–4].

At the same time, a significant portion of the irrigation infrastructure is in unsatisfactory technical condition. The total length of irrigation systems in Kazakhstan exceeds 35,000 km, of which more than 14,000 km are considered to be in critical condition. The average age of many canals exceeds 50 years, while water losses during conveyance through canals reach 40–50%. The main causes include seepage losses, deterioration of concrete lining, crack formation, surface spalling, damage to expansion joints, and the high degree of wear of hydraulic engineering components [1–5].

For the southern regions of Kazakhstan, including the Turkistan Region, Zhambyl Region, Kyzylorda Region, and Almaty Region, the problem is further aggravated by high water salinity, sulfate attack, sharp temperature fluctuations, intense solar radiation, and periodic freezing of canals during winter. As a result of prolonged service life, the concrete lining of canals develops cracks, loses its watertightness, and the hydraulic efficiency of the canals decreases significantly. In some basins of Central Asia, up to 50% of water is lost due to seepage through damaged and cracked canals (Fig. 1).

International experience demonstrates [4–14] that one of the most effective approaches to improving the durability of hydraulic concrete is its modification with various types of dispersed fiber reinforcement. The most commonly used fibers include steel, basalt, polypropylene, glass, and polyvinyl alcohol fibers. The incorporation of fibers makes it possible to significantly reduce shrinkage cracking, increase flexural tensile strength, impact toughness, crack resistance, and resistance to dynamic loading. In addition, fiber reinforcement con-

Fig. 1. Typical defects and cracks in concrete linings of irrigation canals

ISSN 2075-8545 (online)

tributes to limiting the propagation of microcracks, reducing capillary porosity, and decreasing the rate of moisture and aggressive substance penetration into the concrete structure.

Of particular importance for hydraulic structures is the combination of fiber reinforcement with the hydrophobization of high-strength concrete. Hydrophobic admixtures reduce water absorption, capillary suction, and permeability, which is especially critical for irrigation canal linings, where seepage losses directly affect water-use efficiency. International studies indicate that lining deterioration can reduce canal efficiency by up to 25%, while the combined effect of lining degradation and unfavorable hydrogeological conditions may decrease efficiency to as low as 16% [1–12].

Despite the substantial number of studies devoted to fiber-reinforced concrete, the issues related to the combined influence of different fiber types on the physical and mechanical properties, hydrophobicity, chemical resistance, and micro- and nanostructure of high-strength concrete intended for irrigation canal operating conditions in southern Kazakhstan remain insufficiently investigated. Most existing studies focus either on individual fiber types or only on strength characteristics, without considering micro- and nanostructural changes, watertightness, and the behavior of concrete under sulfate attack and cyclic wetting-drying conditions [3-9].

In this regard, the aim of the present study is to evaluate the influence of various types of fiber reinforcement on the physical and mechanical properties, hydrophobicity, and micro- and nanostructure of high-strength concrete intended for irrigation canal linings in the southern regions of Kazakhstan.

To achieve this objective, the following tasks were defined:

1. To develop compositions of high-strength hydrophobic concrete using different types of fibers.

2. To evaluate the influence of fiber reinforcement on compressive, flexural, and tensile strength.

3. To investigate changes in water absorption, watertightness, capillary suction, and hydrophobic properties of concrete.

4. To perform a comparative analysis of the resistance of concrete mixtures to sulfate attack, freeze-thaw cycles, and wetting-drying cycles.

5. To determine the most effective type of fiber reinforcement for improving the durability of irrigation canal linings.

It is expected that the use of hydrophobic high-strength concrete with an optimal type of fiber reinforcement will increase the service life of canal linings by 30–40%, reduce seepage water losses by 15-20%, decrease the intensity of crack formation, and improve the overall operational reliability of hydraulic structures [4–9].

METHODS AND MATERIALS

1. General Research Concept

The study is aimed at evaluating the influence of various types of dispersed fiber reinforcement on the physical and mechanical properties, hydrophobicity, durability, and microstructural features of high-strength concrete intended for irrigation canal linings in the southern regions of Kazakhstan. The experimental program was developed with consideration of the actual operating conditions of irrigation canals, including prolonged water saturation, cyclic wetting and drying, exposure to mineralized water, sulfate attack, abrasive action of water flow, seasonal temperature fluctuations, and the formation of shrinkage and service-induced cracks [13–19].

The study included the following stages [13–19, 21–27]:

1. Development of the base composition of high-strength hydrophobic concrete.

2. Modification of the concrete using various types of fibers.

3. Determination of the physical and mechanical properties of the concrete mixtures.

4. Investigation of hydrophysical properties and hydrophobicity.

5. Evaluation of resistance to sulfate attack, freeze-thaw action, and cyclic wetting-drying.

6. Statistical analysis of the obtained results.

The general research framework is presented in Fig. 2.

2. Raw Materials

High-strength concrete was prepared using Portland cement CEM I 52.5N, quartz sand, crushed granite aggregate, silica fume, a polycarboxylate-based superplasticizer, and an integral hydrophobic admixture of organosilicon origin [13–15, 19–23].

Four types of fibers were used as dispersed reinforcement: steel fiber, basalt fiber, polypropylene fiber, and alkali-resistant glass fiber.

The main characteristics of the materials used are presented in Tables 1 and 2.

3. Concrete Mixture Proportions

The base mixture was designed as a high-strength concrete with a water-to-binder ratio of W/B = 0.28. To increase matrix density and reduce capillary porosity, silica fume was incorporated at 10% of the cement mass. An integral hydrophobic admixture was added at 1.0% of the cement mass. The dosage of the superplasticizer was selected to ensure the required workability of the concrete mixture.

In all experimental mixtures, the volumetric fiber content was 0.5% of the total concrete volume [20–25]. The

ISSN 2075-8545 (online)

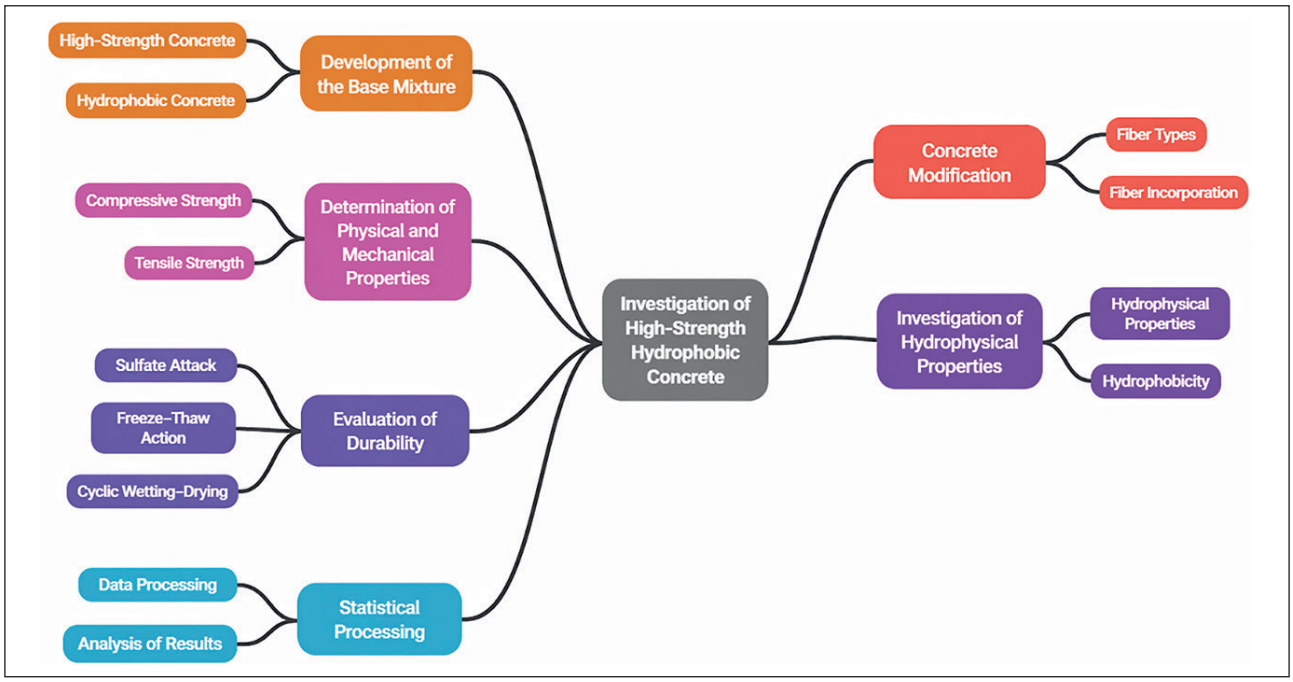

Fig. 2. General research methodology

Table 1. Main characteristics of the raw materials

No.	Material	Characteristic	Value	Material Photo
1	Portland cement	Type	CEM I 52.5N	
2	Portland cement	Cement density	–	
3	Portland cement	Specific surface area	–	
4	Silica fume	Average particle size	Less than 1 μm	
5	Silica fume	Density	–	
6	Quartz sand	Fineness modulus	2.4–2.7	
7	Quartz sand	Density	–	
8	Crushed granite aggregate	Fraction size	5–10 mm	
9	Crushed granite aggregate	Density	–	
10	Superplasticizer	Type	Polycarboxylate-based	
11	Hydrophobic admixture	Type	Organosilicon-based	

ISSN 2075-8545 (online)

Table 2. Characteristics of the fibers used

No.	Fiber Type	Length, mm	Diameter, mm	l/d Ratio	Density, kg/m³	Tensile Strength, MPa	Elastic Modulus, GPa	Material Photo
1	Steel fiber	30	0.50	60	7850	1000–1200	190–210	
2	Basalt fiber	24	0.016–0.020	1200–1500	2650–2700	2800–3200	85–95	
3	Polypropylene fiber	18	0.030–0.040	450–600	910	400–600	3.5–5.0	
4	Alkali-resistant glass fiber	18	0.014–0.020	900–1200	2550–2600	1400–1700	70–75	

Table 3. Compositions of the investigated concrete mixtures, kg/m³

No.	Component	REF	SF	BF	PPF	GF
1	Cement CEM I 52.5N	450	450	450	450	450
2	Silica fume	50	50	50	50	50
3	Water	140	140	140	140	140
4	Sand	720	720	720	720	720
5	Crushed aggregate 5–10 mm	1020	1020	1020	1020	1020
6	Superplasticizer	7.5	7.5	7.5	7.5	7.5
7	Hydrophobic admixture	4.5	4.5	4.5	4.5	4.5
8	Fiber type	–	Steel	Basalt	Polypropylene	Glass
9	Volumetric fiber content, %	0	0.5	0.5	0.5	0.5

Designations of the mixtures: REF – control hydrophobic high-strength concrete without fiber; SF – concrete with steel fiber; BF – concrete with basalt fiber; PPF – concrete with polypropylene fiber; GF – concrete with glass fiber.

control mixture did not contain any fiber reinforcement. The compositions of the concrete mixtures are presented in Table 3. A comparative scheme of the mixture compositions is shown in Fig. 3.

4. Concrete Mixing Procedure and Specimen Preparation

Concrete mixtures were prepared using a laboratory forced-action concrete mixer with a capacity of 60 L. All dry materials were conditioned under laboratory conditions at a temperature of 20 ± 2 °C for at least 24 h prior to mixing. The fibers were pre-divided into small portions to prevent agglomeration and ensure their uniform distribution throughout the mixture volume.

The concrete mixing procedure included the following stages [15–21, 22–26]:

1. Dry mixing of cement, silica fume, sand, and crushed aggregate for 120 s.
2. Addition of 70% of the calculated water content containing the dissolved superplasticizer and hydrophobic admixture.
3. Mixing of the concrete mixture for 180 s.
4. Gradual addition of the remaining water.
5. Introduction of fibers in small portions over 120–180 s.
6. Additional mixing of the mixture for 180 s.

The total mixing duration was 8–10 min. The sequence of the mixing procedure is shown in Fig. 4.

To evaluate the technological properties of the investigated mixtures, the slump of the concrete mix was

ISSN 2075-8545 (online)

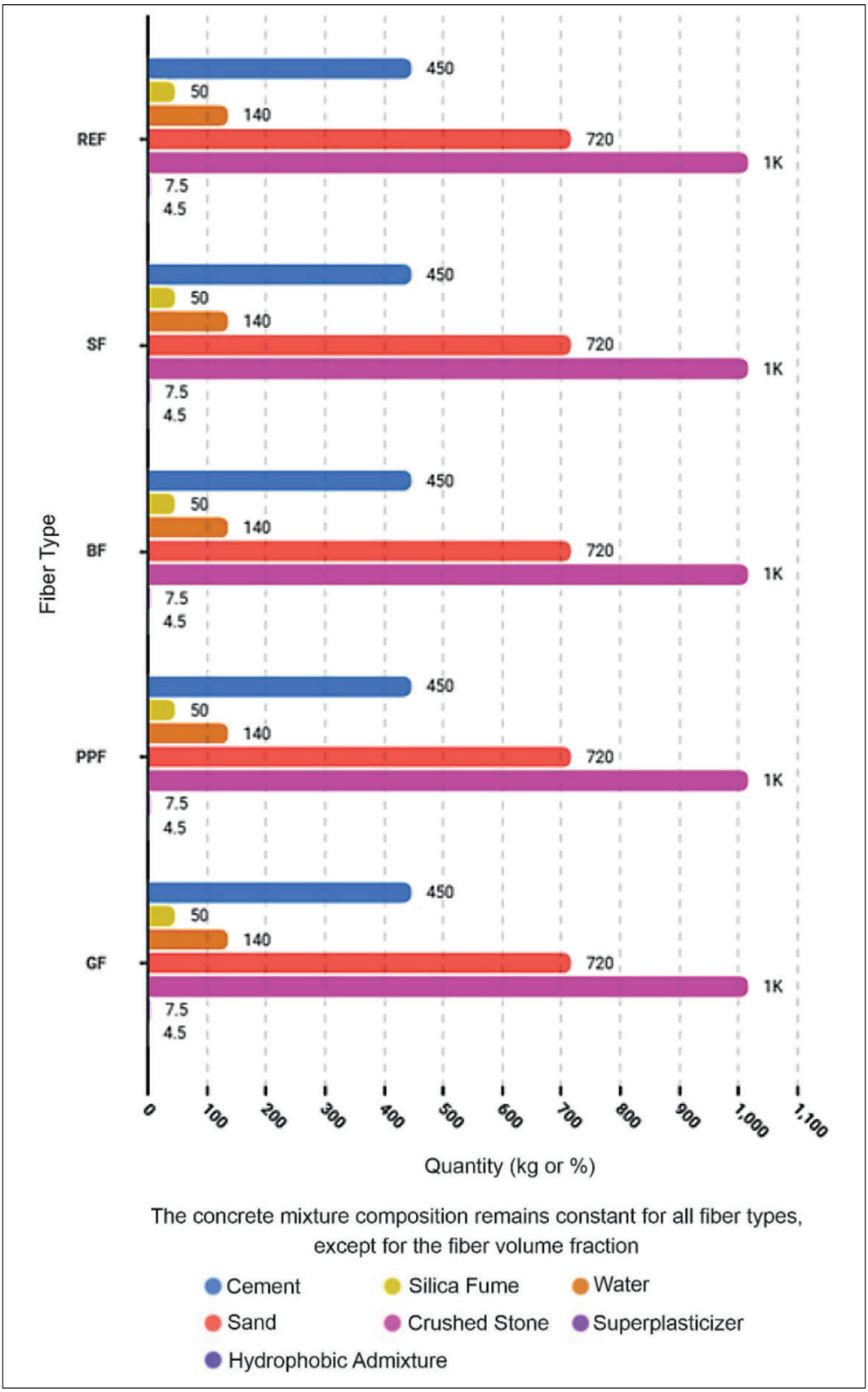

Fig. 3. Comparative scheme of the mixture compositions

ISSN 2075-8545 (online)

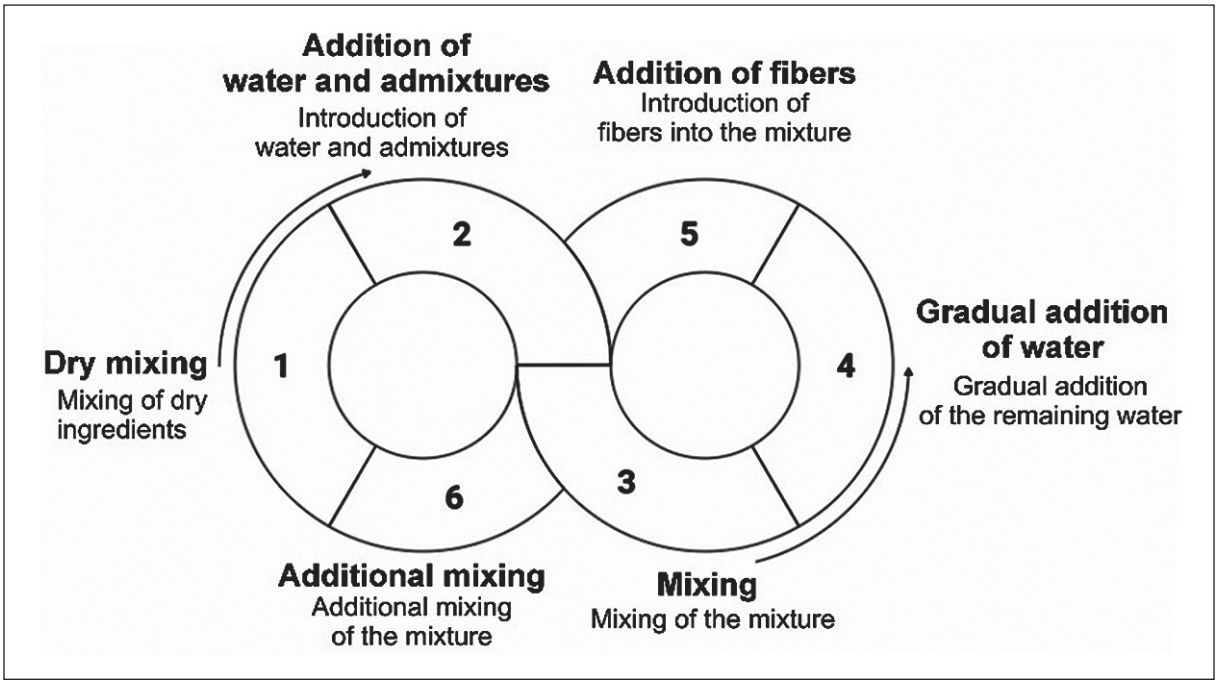

Fig. 4. Concrete mixing cycle

determined in accordance with the requirements of EN 12350-2 [24–30, 31–33]. The tests were performed immediately after completion of the mixing process. Particular attention was paid to the influence of different fiber types on workability, cohesiveness, and the resistance of the concrete mixture to segregation. The characteristic appearance of the concrete mixtures after cone removal is shown in Fig. 5.

As can be seen from Fig. 5, the incorporation of different fiber types had a noticeable effect on the workability of the concrete mixtures. The greatest reduction in slump was observed for the mixtures containing steel and basalt fibers due to the increase in internal friction and the spatial reinforcement effect within the mixture. Polypropylene and glass fibers had a less pronounced effect on workability; however, at increased fiber concentrations, a tendency toward the formation of local fiber agglomerations and reduced mixture homogeneity was observed.

After mixing, the concrete was placed into steel molds and compacted on a vibrating table. The molds were covered with polyethylene film for 24 ± 2 h. After demolding, the specimens were cured at a temperature of 20 ± 2 °C and a relative humidity of 95 ± 5% until reaching the designated testing age.

5. Testing Program

For each mixture, a series of specimens was prepared to ensure the statistical reliability of the results [13–22, 25–27]. At least three parallel specimens were used for physical, mechanical, and hydrophysical tests, while no fewer than five specimens were tested for strength properties. The testing program is presented in Table 4, and the overall scheme of the experimental program is shown in Fig. 6.

6. Methods for Determining Physical and Mechanical Properties

The slump of the concrete mixture was determined immediately after mixing. The target slump value ranged from 50 to 90 mm, corresponding to the conditions required to obtain a dense lining concrete mixture without signs of segregation.

Compressive strength was determined using 100 × 100 × 100 mm cube specimens at the ages of 7, 28, and 90 days [23-25]. Flexural strength was determined on 100 × 100 × 400 mm prism specimens under three-point loading. Splitting tensile strength and elastic modulus were determined using cylindrical specimens measuring 100 × 200 mm.

To evaluate the influence of fiber reinforcement on concrete properties, the relative change in the measured parameters compared with the control mixture was calculated using the following equation [13–16]:

$$\Delta X = \frac{X_i - X_{REF}}{X_{REF}} \cdot 100\%,$$

where X_i – is the value of the parameter for the investigated mixture, and X_{REF} – is the value of the parameter for the control mixture.

ISSN 2075-8545 (online)

Fig. 5. Appearance of the concrete mixtures after the slump test: a – mixture with steel fiber; b – mixture with basalt fiber; c – mixture with polypropylene fiber; d – mixture with glass fiber

Table 4. Testing program

No.	Parameter	Specimen Size	Age / Testing Regime	Number of Specimens
1	Slump	Fresh mixture	Immediately after mixing	3
2	Mixture density	Fresh mixture	Immediately after mixing	3
3	Concrete density	Cube 100×100×100 mm	28 days	3
4	Compressive strength	Cube 100×100×100 mm	7, 28, and 90 days	5
5	Flexural strength	Prism 100×100×400 mm	28 and 90 days	5
6	Splitting tensile strength	Cylinder 100×200 mm	28 days	5
7	Elastic modulus	Cylinder 100×200 mm	28 days	3
8	Water absorption	Cube 100×100×100 mm	28 days	3
9	Capillary absorption	Cube 100×100×100 mm	28 days	3
10	Watertightness	Cube/Cylinder	28 days	3
11	Contact wetting angle	Plate 40×40×10 mm	28 days	3
12	Sulfate resistance	Cube/Prism	30, 90, and 180 days	3
13	Freeze-thaw resistance	Cube/Prism	Up to 300 cycles	3
14	Wetting-drying cycles	Cube/Prism	60 cycles	3

ISSN 2075-8545 (online)

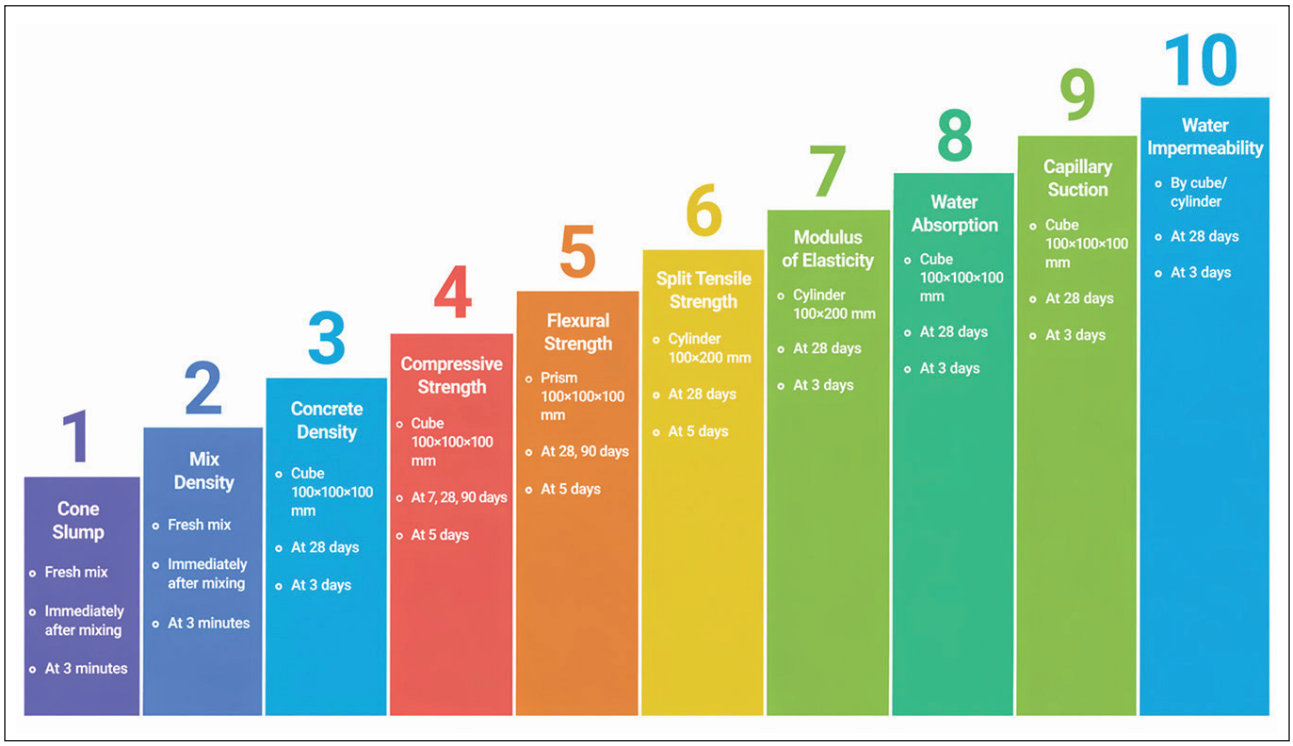

Fig. 6. Scheme of the experimental program

7. Methods for Determining Hydrophobicity and Hydrophysical Properties

Water absorption was determined based on the difference between the masses of dried and water-saturated specimens [27–29]. Water absorption was calculated using the following equation:

$$W_m = \frac{m_{sat} - m_{dry}}{m_{dry}} \cdot 100\%,$$

where m_{sat} – is the mass of the water-saturated specimen, and m_{dry} – is the mass of the dried specimen.

Capillary absorption was determined under conditions of one-sided contact between the specimen and water [33–37]. The mass of the specimens was measured after 10, 30, 60, 120, and 240 min, as well as after 24 and 48 h.

Hydrophobicity was evaluated based on the contact wetting angle [33, 34]. For this purpose, plates measuring 40×40×10 mm were used. A 5 μL drop of deionized water was applied to the surface, and the droplet image was recorded within 5 s. The wetting angle was measured at no fewer than five locations on each specimen.

8. Durability Assessment Methods

Sulfate resistance was evaluated by exposing the specimens to a 5% Na_2SO_4 solution at a temperature of 20 ± 2 °C. The tests were conducted for periods of 30, 90, and 180 days. The solution was renewed every 14 days. After completion of the exposure period, changes in mass, strength, and surface condition were determined [35–39].

Freeze-thaw resistance was evaluated using the method of alternating freezing and thawing under water-saturated conditions. One cycle consisted of freezing at −18 ± 2 °C followed by thawing in water at 20 ± 2 °C. The tests were carried out for up to 300 cycles [28, 32].

To simulate the operating conditions of irrigation canal linings, cyclic wetting-drying tests were performed [1–4, 11]. One cycle included immersing the specimens in water for 8 h followed by drying at a temperature of 50 ± 2 °C for 16 h. The total number of cycles was 60.

RESULTS AND DISCUSSION

1. Technological Properties of Concrete Mixtures

The test results demonstrated that the incorporation of different fiber types significantly affected the technological properties of the high-strength concrete mixtures. All mixtures exhibited a reduction in slump compared with the control mixture REF, which is associated with increased internal friction within the mixture and the higher specific surface area of the dispersed reinforcement.

The greatest reduction in workability was observed for the steel fiber-reinforced mixture (SF), where the slump value was 64 mm compared with 82 mm for the control mixture. This behavior can be attributed to the high stiffness, density, and developed surface area of

ISSN 2075-8545 (online)

the steel fibers. The mixture containing basalt fiber (BF) was also characterized by a noticeable reduction in slump to 68 mm. Polypropylene and glass fibers had a less pronounced effect on the mobility of the concrete mixture.

Despite the reduction in workability, all mixtures maintained satisfactory technological performance, exhibited no signs of segregation, and ensured a uniform distribution of fibers throughout the mixture volume. The use of the superplasticizer made it possible to maintain the slump within a range suitable for the production of concrete linings for irrigation canals. The results are presented in Fig. 7.

2. Compressive, Flexural, and Splitting Tensile Strength

The incorporation of fibers contributed to an improvement in all investigated strength characteristics of concrete. However, the magnitude of the improvement depended on the type of reinforcement used. The histogram shown in Fig. 8 presents the physical and mechanical properties of the investigated concrete mixtures containing different types of fiber reinforcement. The analysis of the results indicates that all fiber types improved the strength and deformation characteristics of concrete compared with the control mixture REF.

The highest compressive strength values at both 28 and 90 days were obtained for the steel fiber-reinforced mixture SF, where the strength reached 79.6 and 85.9 MPa, respectively. This can be explained by the high stiffness and tensile strength of steel fibers, which effectively resist tensile stresses and inhibit crack propagation.

Basalt fiber-reinforced concrete (BF) also demonstrated high efficiency, providing an increase in compressive strength of 12.3% and an increase in flexural strength of 33.3%. Polypropylene fiber-reinforced concrete (PPF) exhibited a smaller increase in strength; however, its use improved crack resistance and reduced the risk of brittle failure through the formation of a large number of fine distributed cracks. Glass fiber-reinforced concrete (GF) showed intermediate performance between BF and PPF, demonstrating a stable increase in flexural strength and elastic modulus.

The highest values of flexural strength, splitting tensile strength, and elastic modulus were also recorded for mixture SF, where these parameters reached 11.2 MPa, 6.4 MPa, and 43.8 GPa, respectively. This indicates that steel fiber is the most effective in enhancing the resistance of concrete to crack initiation and propagation, as well as increasing its stiffness and ability to withstand dynamic and impact loading.

Figure 9 presents the characteristic failure patterns of concrete cubes reinforced with different types of fibers after axial compression testing. In all cases, failure was accompanied by the formation of vertical and inclined cracks propagating from the central zone of the specimen toward its lateral surfaces. For the fiber-reinforced speci-

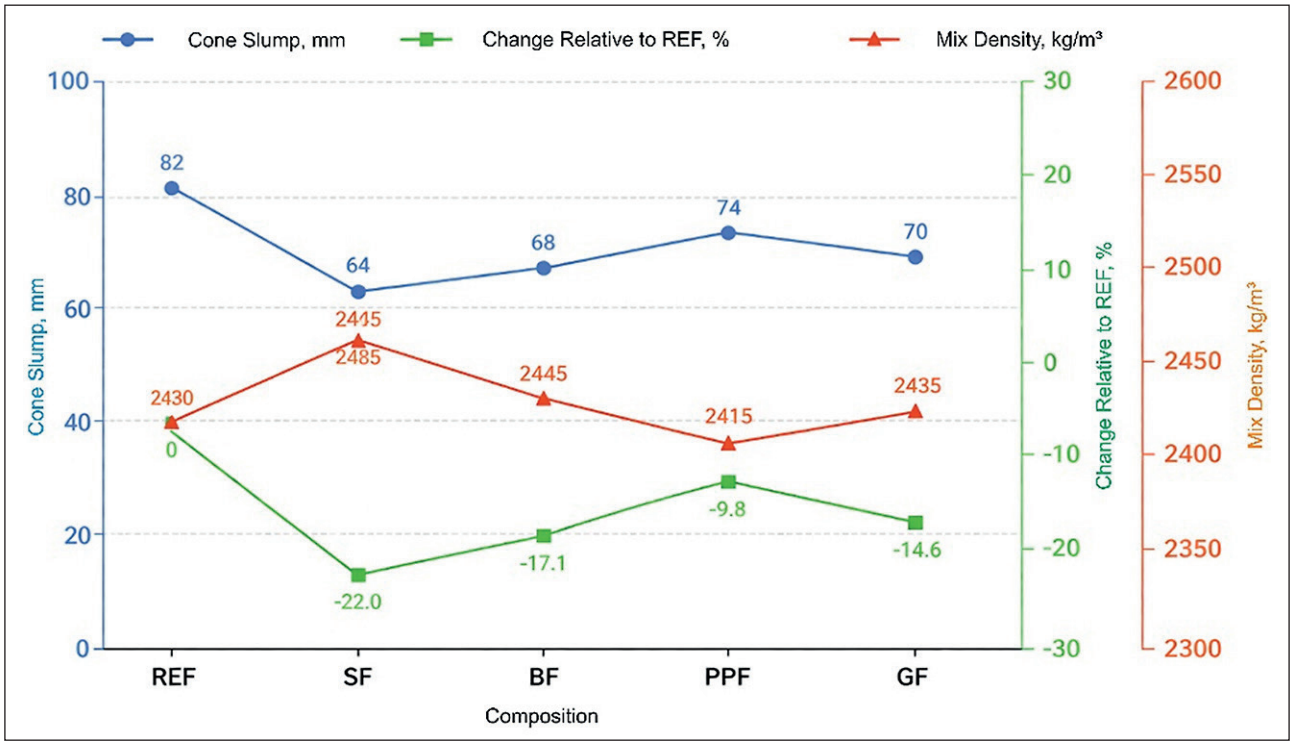

Fig. 7. Technological properties of the concrete mixtures

ISSN 2075-8545 (online)

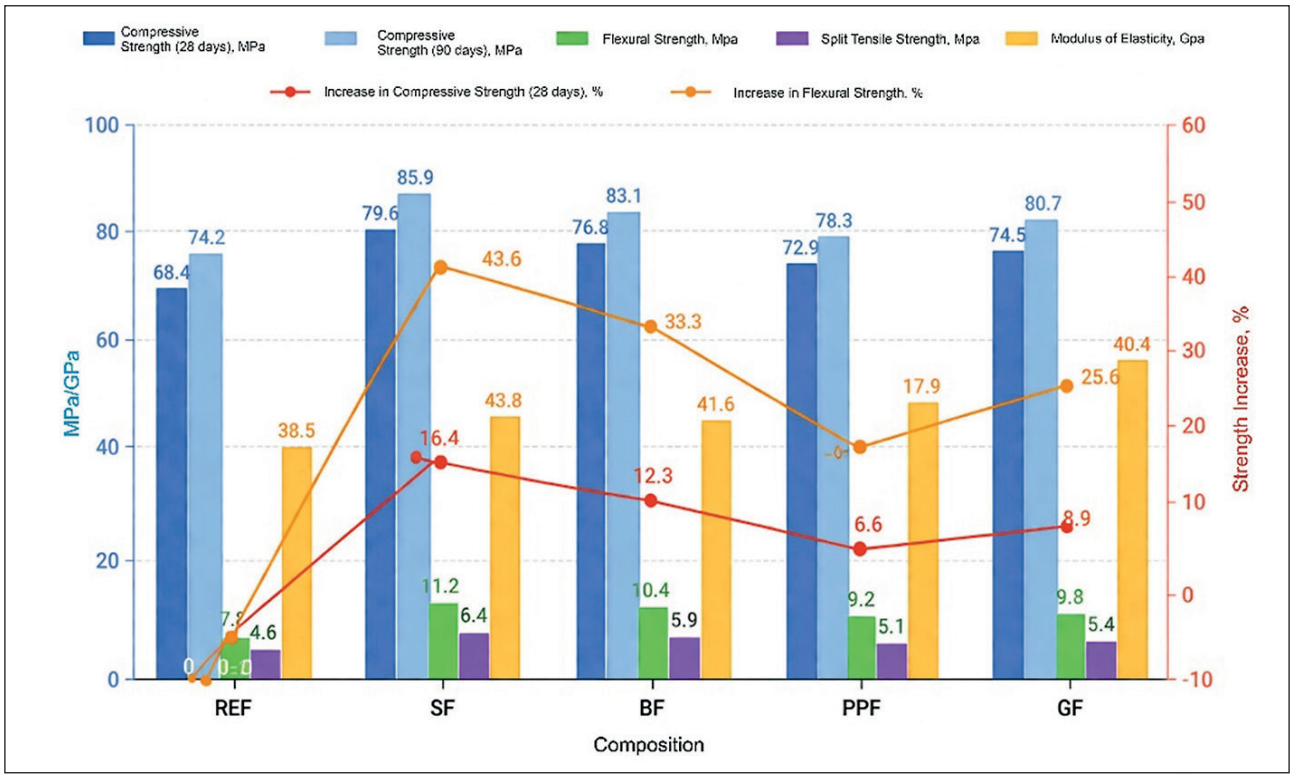

Fig. 8. Physical and mechanical properties of the investigated concrete mixtures

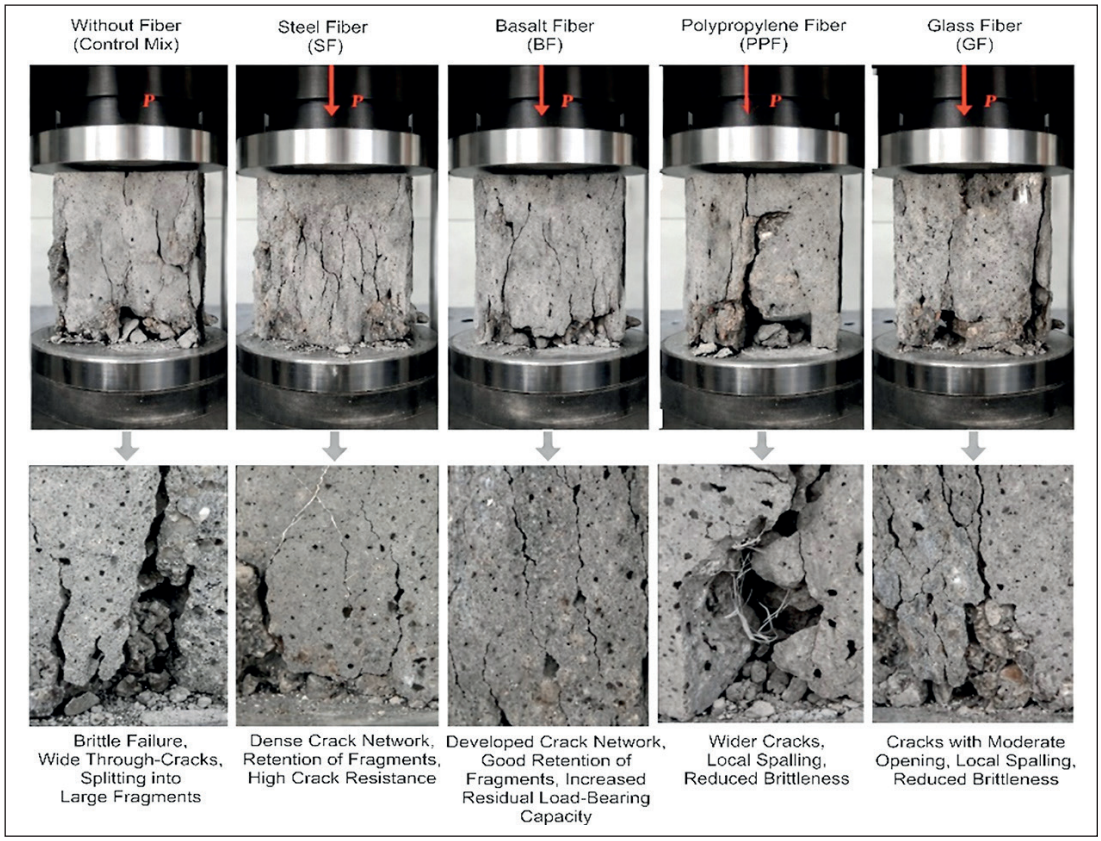

Fig. 9. Failure patterns of concrete specimens with different types of fiber reinforcement under axial compression testing

ISSN 2075-8545 (online)

mens, the overall integrity of the concrete was preserved even after reaching the ultimate load.

In the specimens containing steel and basalt fibers, a more pronounced three-dimensional crack network was observed, accompanied by the retention of individual concrete fragments, indicating improved crack resistance and residual load-bearing capacity of the material. Polypropylene and glass fibers also contributed to reducing the intensity of brittle failure; however, in these cases, greater crack opening and local spalling of the cement matrix in the loading zone were observed.

As shown in Table 5, the highest compressive strength of the cube specimens was achieved for the steel fiber-reinforced mixture SF, reaching 79.6 MPa, which is 16.4% higher than that of the control mixture. Basalt fiber also provided a significant increase in strength, up to 76.8 MPa. Specimens containing polypropylene and glass fibers showed a more moderate improvement in strength; however, in all cases, a change in the failure mechanism compared with the control mixture was observed.

Figure 10 presents the characteristic crack patterns observed in concrete beams with different ratios of steel and polypropylene fibers after flexural testing. In all specimens, the formation of a main vertical crack in the central span region was observed, corresponding to the zone of maximum tensile stresses.

Figure 10a shows the specimen with a predominance of steel fiber (SF/PPF = 75/25). This mixture is characterized by the formation of a single narrow major crack with limited crack opening. This behavior is associated with the high ability of steel fibers to resist tensile stresses and restrict the propagation of the primary crack.

Figure 10b presents the specimen with a balanced content of steel and polypropylene fibers (SF/PPF = 50/50). In this case, a primary crack with moderate opening was observed, together with the development of additional secondary cracks in the central span region. Such a failure pattern indicates a more uniform redistribution of stresses within the material.

Figure 10c shows the specimen with a predominance of polypropylene fiber (SF/PPF = 25/75). This specimen is characterized by the formation of a branched crack network with larger crack openings and gradual damage development. An increase in the proportion of polypropylene fiber contributes to improved deformability and reduced brittleness of failure; however, it is accompanied by more pronounced crack development.

Figure 11 presents the characteristic stages of crack development in concrete beams during flexural testing. In all cases, failure initiated in the central span region, where the maximum tensile stresses occur.

Figure 11a shows the initial stage of failure under a relatively low load level. A vertical crack forms in the lower tensile zone of the beam and propagates upward through the cross-section. At this stage, the crack opening width remains limited, and most of the beam retains its structural integrity.

Figure 11b presents the stage of active loading, accompanied by the opening and further propagation of the primary crack. It can be seen that damage is concentrated mainly in the central part of the beam. During this stage, instrumental monitoring of crack opening is performed, making it possible to assess changes in crack width throughout the loading process.

Figure 11c shows the final stage of failure under the ultimate load. This stage is characterized by the formation of a well-developed major crack extending through the entire beam cross-section. In the failure zone, local spalling of the cement matrix, partial exposure of coarse aggregate, and an increase in crack opening width are observed.

Figure 12 presents a comparative histogram of flexural strength, failure load, relative strength increase, and main crack opening width for the investigated concrete mixtures.

Table 5. Results of axial compression tests on cube specimens

No.	Mixture	Failure Load, kN	Relative Change Compared with REF, %	Failure Pattern	Visual Integrity after Failure
1	REF	684	–	Brittle failure with the formation of major vertical and inclined cracks	Low
2	SF	796	+16.4	Cracks develop gradually, with retention of fragments due to steel fibers	High
3	BF	768	+12.3	Failure is less brittle, with a pronounced limitation of crack opening	High
4	PPF	729	+6.6	A network of finer cracks is formed, resulting in a less severe failure mode	Medium
5	GF	745	+8.9	Crack formation is localized, and the integrity of the specimen is partially preserved	Medium-high

ISSN 2075-8545 (online)

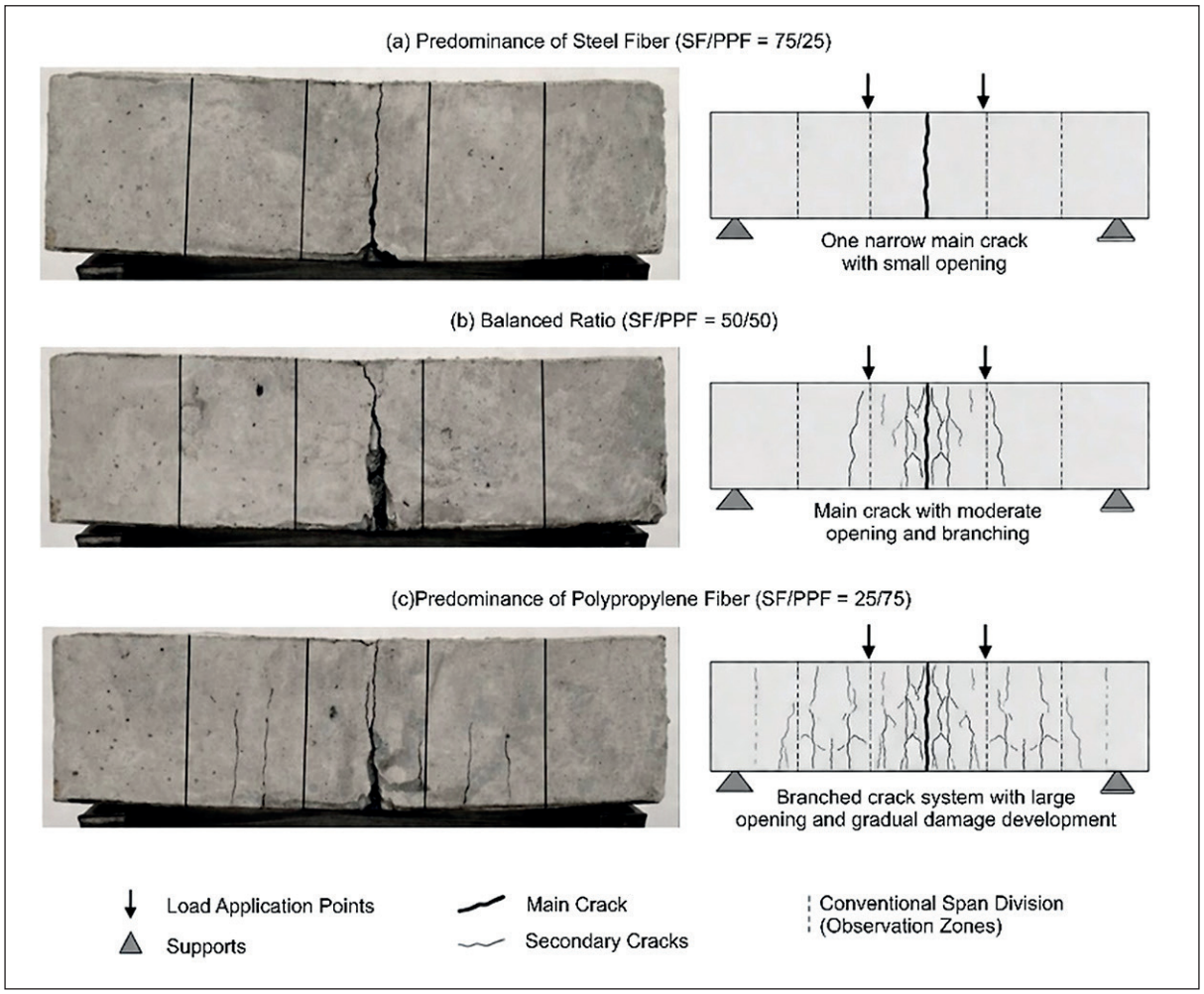

Fig. 10. Crack patterns in concrete beams with different ratios of steel and polypropylene fibers after flexural testing

It was found that the highest values of flexural strength and failure load were achieved for the steel fiber-reinforced mixture. The flexural strength increased from 7.8 MPa for the control mixture REF to 11.2 MPa for mixture SF, while the failure load increased from 17.3 to 24.9 kN. The mixture containing basalt fiber also demonstrated high performance, with a flexural strength of 10.4 MPa and a failure load of 23.1 kN.

The greatest relative increase in strength compared with the control mixture was observed for SF and reached +43.6%, whereas for BF this value was +33.3%. For the mixtures containing polypropylene and glass fibers, the increase in strength was less pronounced and amounted to +17.9% and +25.6%, respectively.

At the same time, the incorporation of fibers contributed to a significant reduction in the opening width of the major crack. While this value was 0.95 mm for the control mixture REF, it decreased to 0.42 mm for SF and to 0.48 mm for BF. For the mixtures containing polypropylene and glass fibers, the crack opening width was 0.61 and 0.56 mm, respectively.

The failure load was calculated according to the three-point bending scheme:

$$R_{flex} = \frac{3PL}{2bh^2},$$

where $L = 100$ mm, $b = 100$ mm, and $h = 100$ mm.

Figure 13 presents the characteristic failure patterns of cylindrical concrete specimens with different types of fiber reinforcement after axial compression testing: (a) REF – control mixture without fiber; (b) SF – mixture with steel fiber; (c) BF – mixture with basalt fiber; (d) PPF – mixture with polypropylene fiber; (e) GF – mixture with glass fiber.

The control mixture REF was characterized by the formation of a wide major vertical crack accompanied by intensive spalling of the cement matrix and partial destruction of the protective concrete layer. The failure exhibited a distinctly brittle character and was accompanied by rapid separation of the specimen into individual fragments.

In the specimens containing steel fiber, limitation of the main crack opening and retention of individual

ISSN 2075-8545 (online)

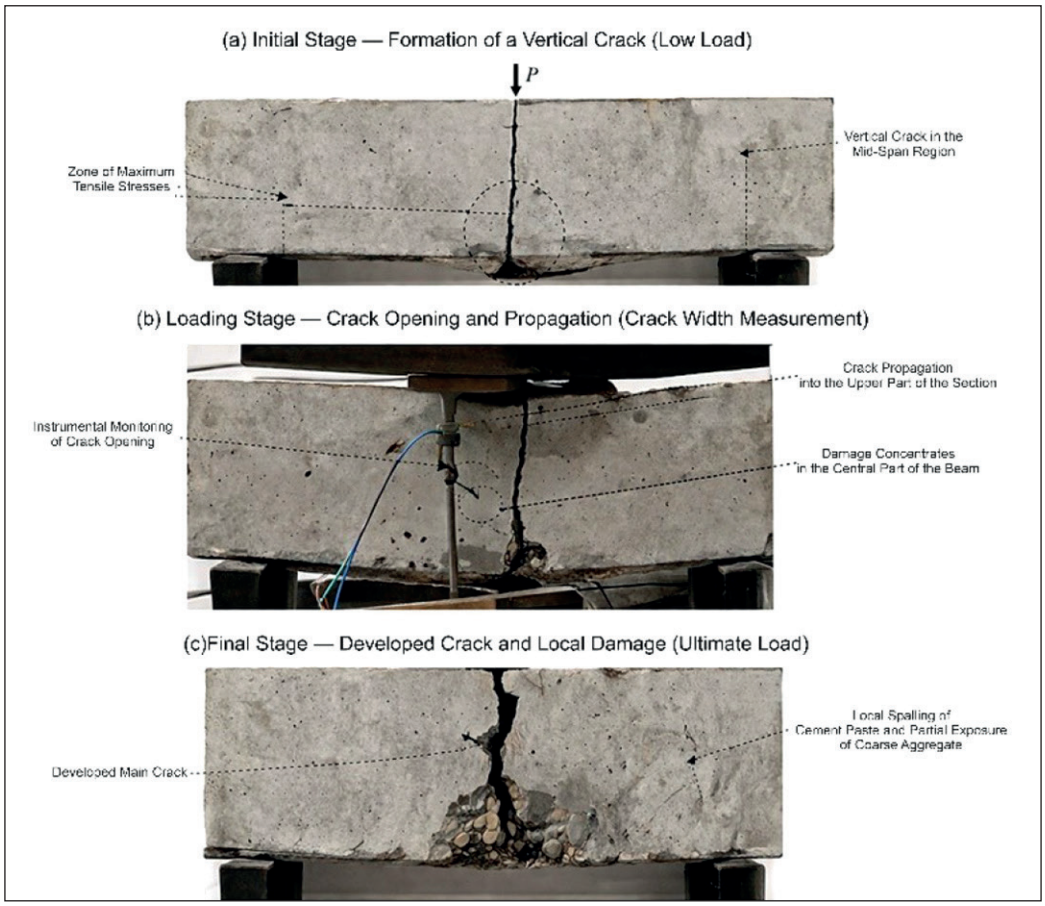

Fig. 11. Development of cracks and opening of the major crack in concrete beams during flexural testing

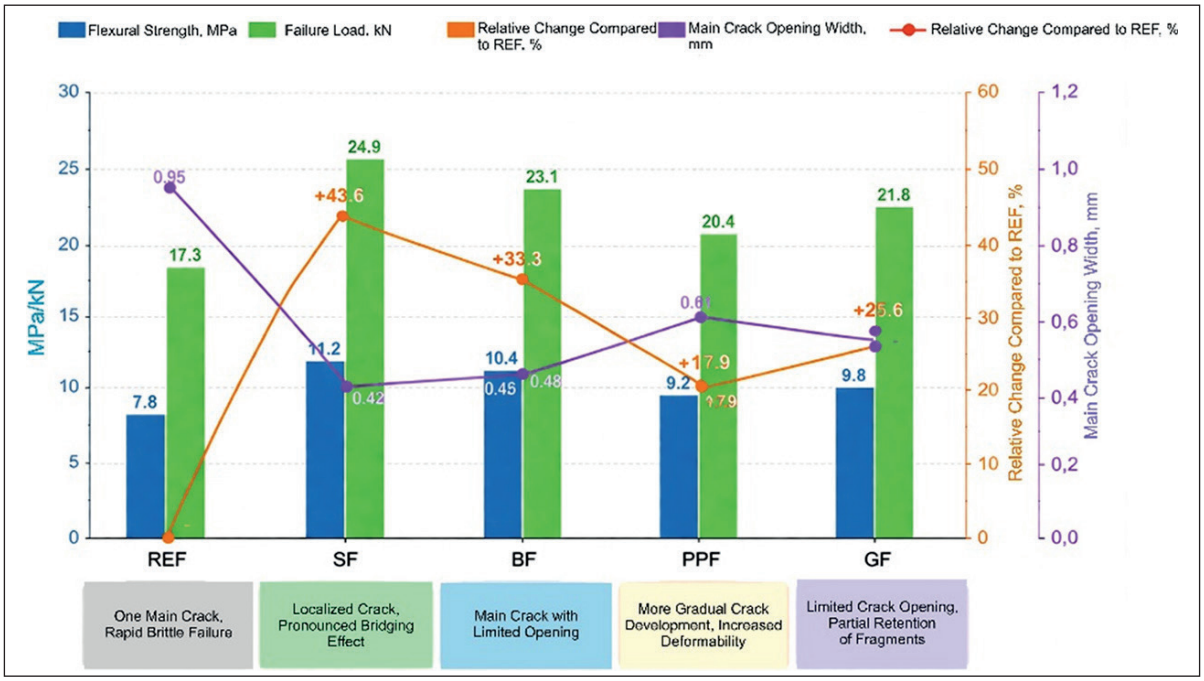

Fig. 12. Comparison of flexural strength and crack resistance of concrete mixtures with different types of fiber reinforcement

ISSN 2075-8545 (online)

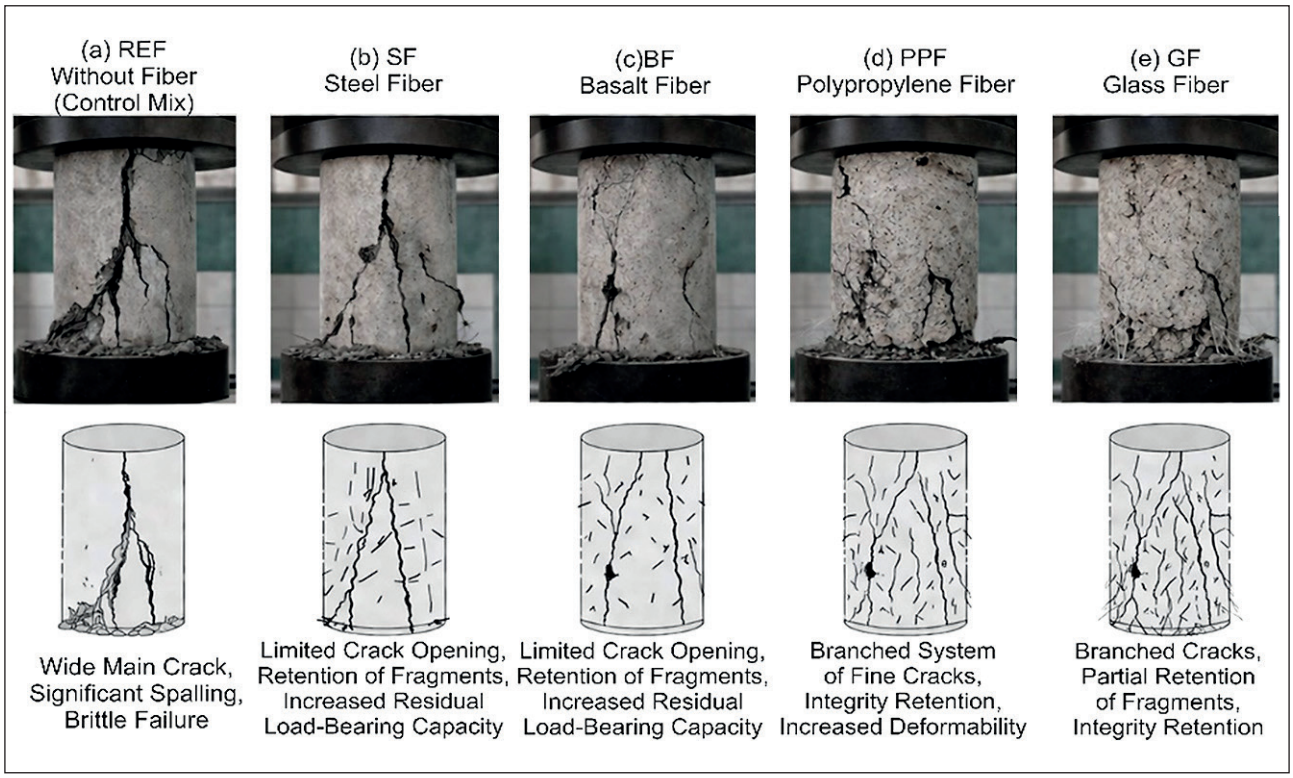

Fig. 13. Characteristic failure patterns of cylindrical concrete specimens under axial compression: a – REF – without fiber; b – SF – steel fiber; c – BF – basalt fiber; d – PPF – polypropylene fiber; e – GF – glass fiber

concrete fragments after reaching the ultimate load were observed. The fibers prevented complete failure of the cylinder and ensured the preservation of residual load-bearing capacity.

Mixtures containing basalt fiber were also characterized by limited crack opening and retention of concrete fragments. However, compared with steel fiber, the cracks exhibited a more pronounced branched pattern, indicating gradual damage development and enhanced deformability of the material.

The specimens reinforced with polypropylene fiber were characterized by the formation of an extensive network of fine cracks with a relatively small amount of local spalling. The fibers contributed to maintaining the integrity of the cylinder and prevented complete disintegration of the specimen even after reaching the ultimate state.

For the mixtures containing glass fiber, the formation of a large number of fine and medium-sized cracks was observed, accompanied by partial retention of concrete fragments by the fibers. Despite the presence of local damage, the overall shape of the specimen was preserved, indicating an increase in residual strength and resistance to progressive failure.

Figure 14 presents the characteristic failure patterns of concrete specimens during pull-out testing: (a) REF – control mixture without fiber; (b) SF – mixture with steel fiber; (c) BF – mixture with basalt fiber; (d) PPF – mixture with polypropylene fiber; (e) GF – mixture with glass fiber.

In all cases, failure initiated in the zone of concentrated load application and was accompanied by the formation of a conical breakout surface, the development of radial cracks, and local spalling of the cement matrix. As the load increased, a damaged core gradually formed beneath the loaded element, followed by the separation of individual concrete fragments.

The control mixture REF (Fig. 14a) exhibited the most intensive and brittle failure pattern. A wide breakout zone, a significant number of radial cracks, and the separation of large concrete fragments were observed. The damaged core had a pronounced character, indicating the low ability of the material to resist localized tensile stresses after reaching the ultimate load.

In the specimens reinforced with steel fiber SF (Fig. 14b), the failure pattern was more localized. Steel fibers limited the opening of radial cracks and retained the damaged concrete fragments due to a pronounced bridging effect. This contributed to an increase in residual load-bearing capacity and a reduction in brittle failure intensity.

The mixtures containing basalt fiber BF (Fig. 14c) were also characterized by limited development of the breakout zone and moderate separation of concrete fragments. Basalt fiber contributed to reducing crack opening

ISSN 2075-8545 (online)

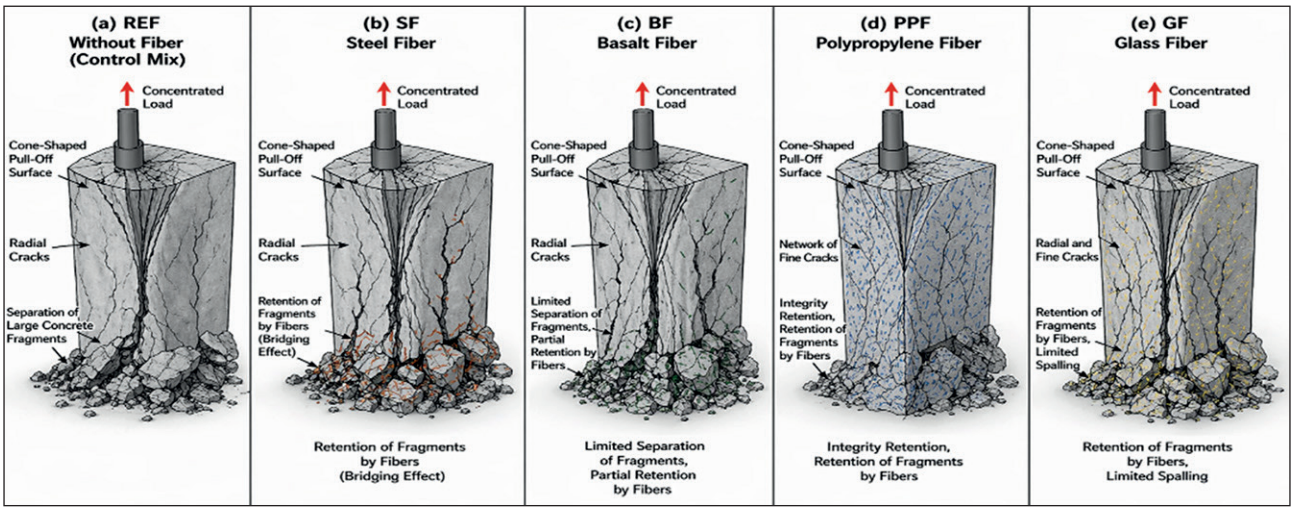

Fig. 14. Characteristic failure patterns of concrete specimens during pull-out testing: a – REF – without fiber; b – SF – steel fiber; c – BF – basalt fiber; d – PPF – polypropylene fiber; e – GF – glass fiber

width and partially retaining the damaged material in the pull-out zone.

The specimens reinforced with polypropylene fiber PPF (Fig. 14d) were characterized by the formation of a more developed network of fine cracks with a smaller amount of local spalling. In this case, failure developed more gradually, while the fibers prevented complete separation of fragments and contributed to preserving the integrity of the specimen.

For the mixtures containing glass fiber GF (Fig. 14e), a combination of radial and fine cracks, limited spalling, and partial retention of damaged fragments by the fibers was observed. Despite the presence of local damage, the specimen retained its overall integrity and ability to carry load after reaching the ultimate state.

According to the data presented in Table 6, the use of fiber reinforcement contributed to an increase in the resistance of concrete to localized pull-out failure. The highest maximum pull-out load was recorded for the steel fiber-reinforced mixture SF and reached 56.8 kN, which is 33.6% higher than that of the control mixture REF. For the mixture containing basalt fiber BF, the maximum load reached 52.9 kN, while the increase relative to REF was 24.5%.

It was found that the incorporation of fibers led to a reduction in the dimensions of the damaged core and the diameter of the breakout zone. For the control mixture REF, the depth of the damaged core was 58 mm, while the breakout zone diameter was 142 mm. In the specimens reinforced with steel fiber, these values decreased to 46 and 118 mm, respectively, indicating a more localized failure pattern.

For the mixtures containing polypropylene and glass fibers, a reduction in the size of the damaged zone was also observed; however, the main effect of these fiber types was manifested in the reduced intensity of spalling and the retention of individual concrete fragments after reaching the ultimate load.

Table 6. Pull-out resistance parameters of concrete with different types of fiber reinforcement

No.	Mixture	Maximum Pull-Out Load, kN	Relative Change Compared with REF, %	Depth of Damaged Core, mm	Breakout Zone Diameter, mm	Failure Pattern
1	REF	42.5	–	58	142	Wide breakout zone, intensive spalling, separation of large fragments
2	SF	56.8	+33.6	46	118	Localized failure, pronounced bridging effect, retention of fragments
3	BF	52.9	+24.5	49	124	Limited crack opening, moderate fragment separation
4	PPF	48.7	+14.6	52	130	Developed network of fine cracks, preservation of integrity
5	GF	50.3	+18.4	50	127	Limited spalling, partial retention of damaged fragments

ISSN 2075-8545 (online)

Figure 15 shows the influence of different combinations of steel and polypropylene fibers on the compressive strength and elastic modulus of cylindrical concrete specimens. With increasing steel fiber content and the addition of polypropylene fiber, a stable trend toward improved concrete strength and stiffness was observed. The highest values were achieved for the mixture containing SF0.7% + PPF0.3%, whereas the control specimen without fibers exhibited the lowest values. The graph demonstrates the effectiveness of hybrid fiber reinforcement, which provides greater resistance of the specimens to external loading and improves their deformation stability.

3. Water Absorption, Capillary Absorption, and Hydrophobicity

For irrigation canal linings, particular importance is attached to the parameters characterizing permeability and the ability of concrete to resist water penetration. The results showed that all fiber types, in combination with the hydrophobic admixture, contributed to reducing water absorption and capillary moisture transport.

Figure 16 presents a multi-axis histogram of the hydrophysical properties of the investigated concretes, including water absorption, reduction in water absorption relative to the control mixture, capillary absorption coefficient, contact angle, and watertightness grade.

It was found that the use of fiber reinforcement contributed to reducing the water absorption of concrete. The lowest value of this parameter was observed for the steel fiber-reinforced mixture SF and amounted to 3.41%, which is 29.3% lower than that of the control mixture REF. For the basalt fiber-reinforced mixture BF, water absorption was 3.56%, while the reduction relative to REF reached 26.1%. For the mixtures containing polypropylene and glass fibers, this parameter was 3.94% and 3.78%, respectively.

A similar trend was observed for the capillary absorption coefficient. For the control mixture REF, this parameter was 0.184 kg/(m²·h^0.5), whereas for SF and BF it decreased to 0.121 and 0.129 kg/(m²·h^0.5), respectively. This indicates a reduction in the intensity of capillary moisture transport and an increase in the density of the concrete structure.

At the same time, an increase in the surface contact angle of concrete was observed. For REF, the contact angle was 84°, whereas for SF it increased to 101° and for BF to 98°. The increase in contact angle indicates enhanced surface hydrophobicity and a reduced tendency of concrete to be wetted by water.

The highest watertightness grades were also achieved for the mixtures containing steel and basalt fibers. For REF, the watertightness grade was W10, whereas for SF and BF it increased to W14. For the mixtures containing polypropylene and glass fibers, a watertightness grade of W12 was obtained.

4. Resistance to Sulfate Attack

Figure 17 presents a multi-axis histogram of the sulfate resistance parameters of the investigated concrete mix-

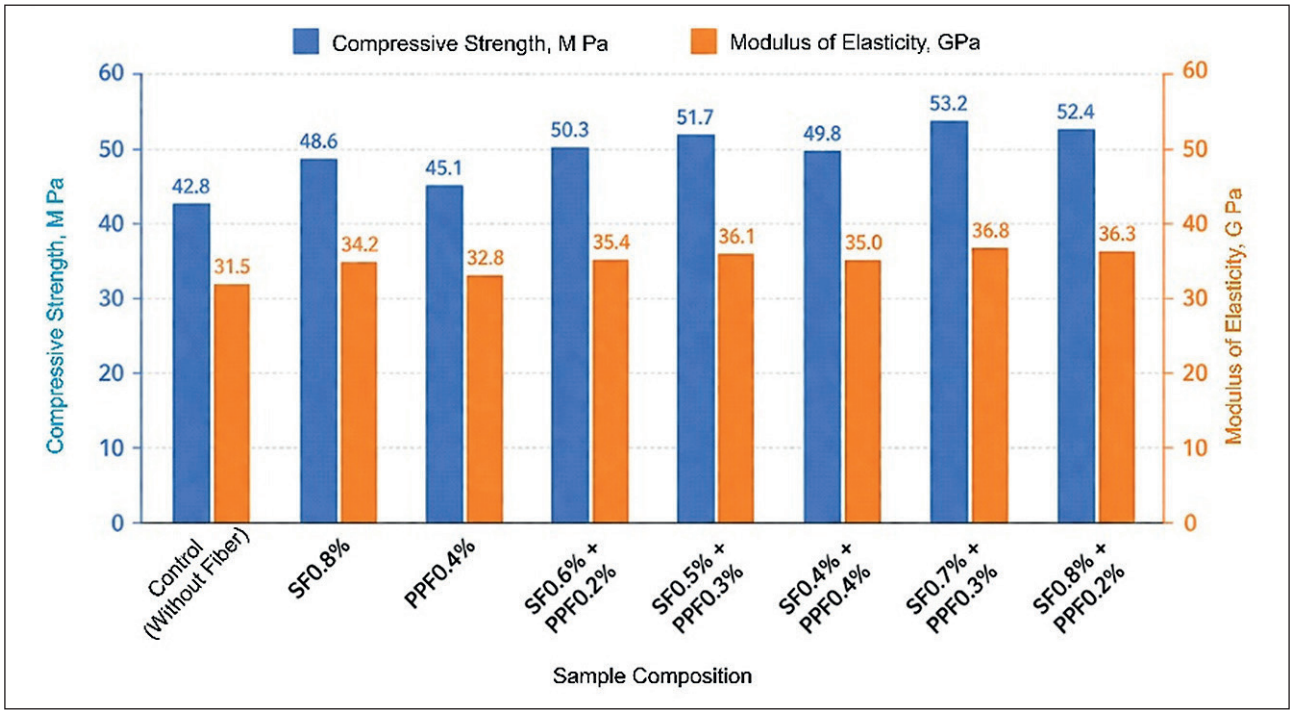

Fig. 15. Results of axial compression and elastic modulus tests on cylindrical concrete specimens

ISSN 2075-8545 (online)

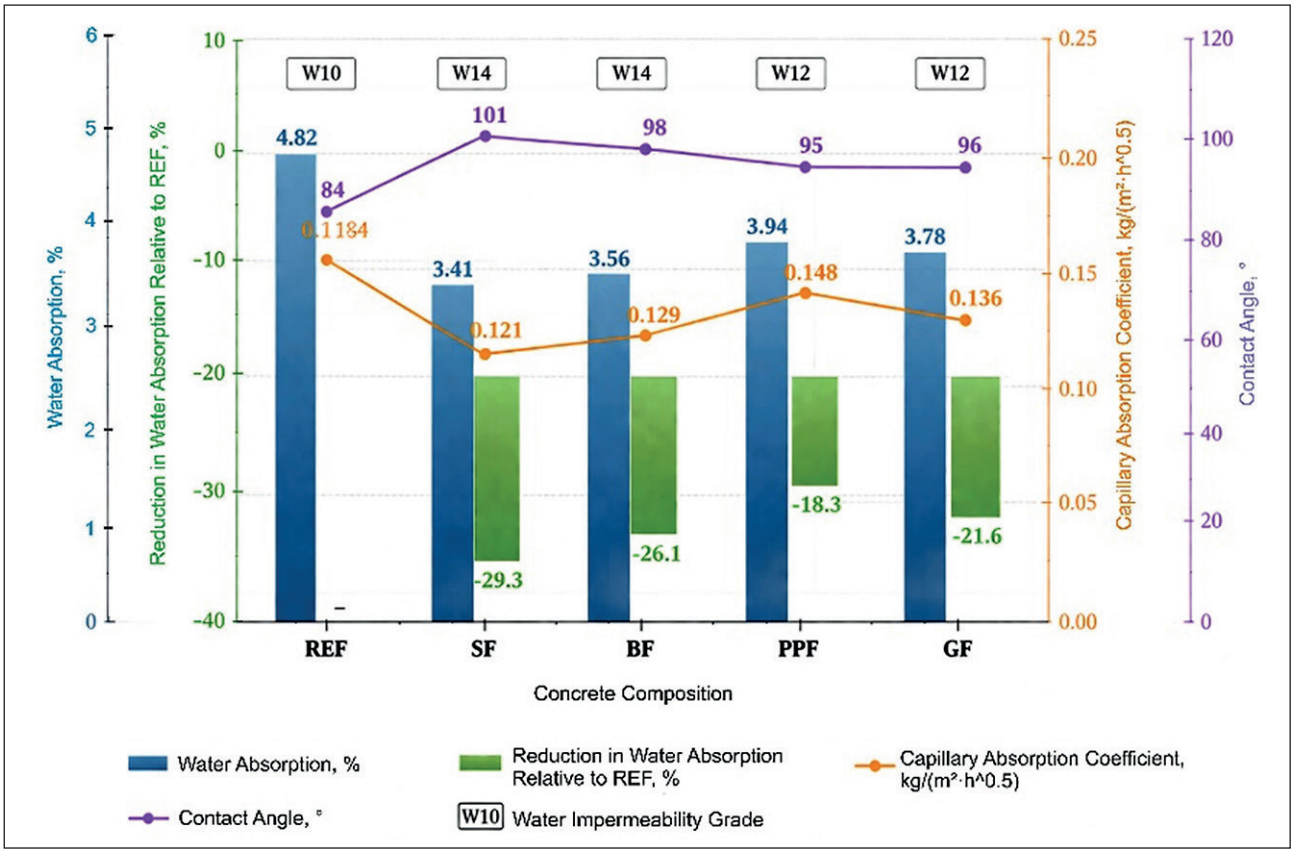

Fig. 16. Hydrophysical properties of the investigated concrete mixtures

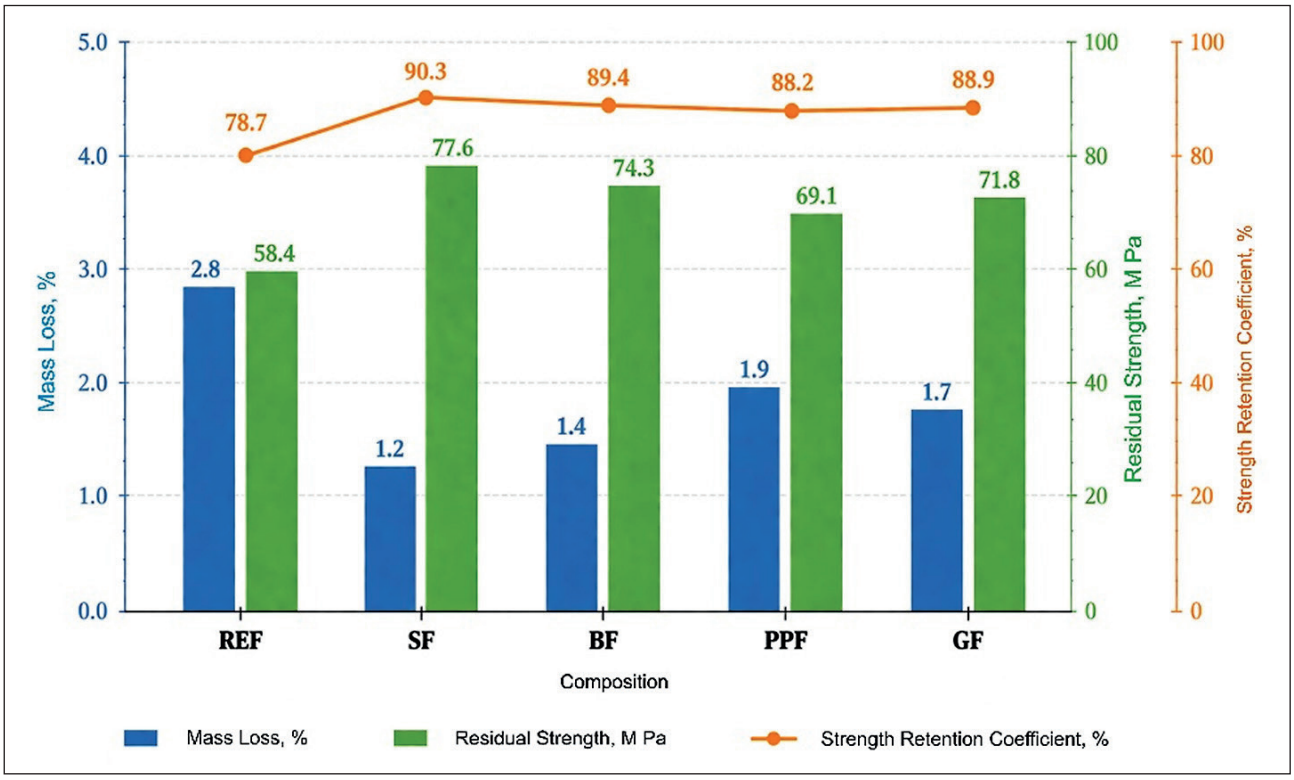

Fig. 17. Sulfate resistance parameters after 180 days

ISSN 2075-8545 (online)

tures after 180 days of exposure to an aggressive sulfate environment. The figure includes the values of mass loss, residual strength, and strength retention coefficient for the control mixture and concretes reinforced with different types of fibers.

It was found that the control mixture REF exhibited the highest mass loss of 2.8%, indicating the most intensive development of sulfate corrosion processes. The incorporation of fibers made it possible to significantly reduce this parameter. The minimum mass loss was observed for the steel fiber-reinforced mixture SF and amounted to 1.2%, whereas for BF this value was 1.4%, for GF it was 1.7%, and for PPF it was 1.9%.

The residual strength after 180 days of exposure to the sulfate environment was 58.4 MPa for the control mixture REF. The use of fiber reinforcement ensured a noticeable increase in this parameter. The highest residual strength was recorded for mixture SF at 77.6 MPa. For BF, the residual strength was 74.3 MPa; for GF, it was 71.8 MPa; and for PPF, it was 69.1 MPa.

A similar trend was observed for the strength retention coefficient. For the REF mixture, this parameter was 78.7%, whereas for the fiber-reinforced mixtures it increased to 90.3% for SF, 89.4% for BF, 88.9% for GF, and 88.2% for PPF.

5. Freeze-Thaw Resistance and Resistance to Wetting-Drying Cycles

Figure 18 presents a histogram of the freeze-thaw resistance and resistance of the investigated concrete mixtures to wetting-drying cycles. The figure includes the values of mass loss after 300 freeze-thaw cycles, strength reduction after 300 cycles, and residual strength after 60 wetting-drying cycles.

The control mixture REF exhibited the highest mass loss after 300 freeze-thaw cycles, amounting to 4.6%. At the same time, it also showed the greatest reduction in strength, equal to 18.4%. This indicates the most intensive deterioration of the concrete structure under cyclic freezing and subsequent thawing.

The incorporation of fibers significantly improved the freeze-thaw resistance of concrete. The lowest mass loss was recorded for the steel fiber-reinforced mixture SF at 1.8%, whereas for BF this value was 2.1%, for GF it was 2.4%, and for PPF it was 2.8%. A similar trend was observed for the reduction in strength after 300 cycles: the minimum strength reduction was recorded for SF at 7.6%, while for BF it was 8.9%, for GF it was 9.8%, and for PPF it was 10.7%.

High values of residual strength after 60 wetting-drying cycles were also characteristic of fiber-reinforced concrete. For REF, the residual strength was 79.2%, whereas for SF it increased to 92.5%, for BF to 91.3%, for GF to 89.7%, and for PPF to 88.4%.

CONCLUSION

Based on the conducted research, the following conclusions can be drawn:

1. The incorporation of dispersed fibers increased the 28-day compressive strength of concrete by 6.6–

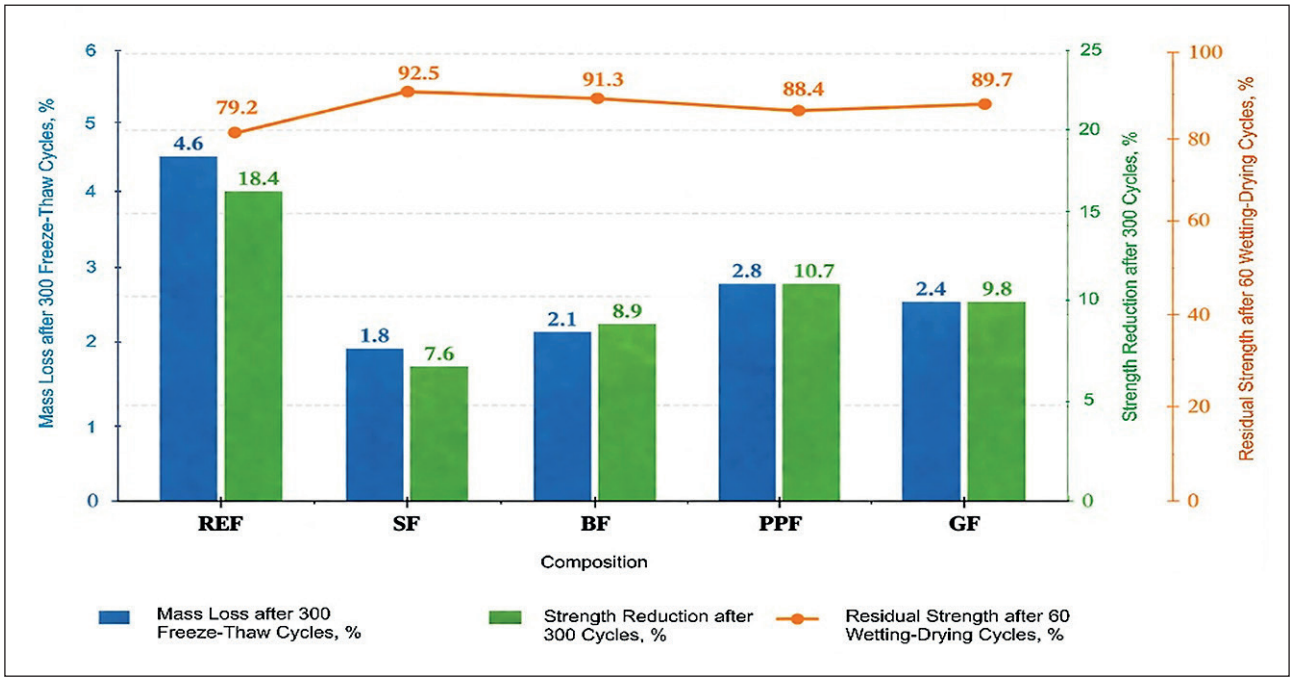

Fig. 18. Freeze-thaw resistance and resistance to wetting-drying cycles

ISSN 2075-8545 (online)

16.4% compared with the control mixture REF. The highest strength was obtained for mixture SF, reaching 79.6 MPa, which is 16.4% higher than the control mixture (68.4 MPa). For mixture BF, the compressive strength was 76.8 MPa (+12.3%); for GF, 74.5 MPa (+8.9%); and for PPF, 72.9 MPa (+6.6%).

2. At the age of 90 days, the highest strength values were also recorded for mixtures SF and BF. The compressive strength of SF reached 85.9 MPa, BF reached 83.1 MPa, GF reached 80.7 MPa, and PPF reached 78.3 MPa, whereas for REF this parameter was 74.2 MPa.

3. The most pronounced effect of fiber reinforcement was observed under flexural loading. Flexural strength increased from 7.8 MPa for REF to 11.2 MPa for SF (+43.6%), 10.4 MPa for BF (+33.3%), 9.8 MPa for GF (+25.6%), and 9.2 MPa for PPF (+17.9%).

4. Splitting tensile strength also increased in all reinforced mixtures: from 4.6 MPa for REF to 6.4 MPa for SF, 5.9 MPa for BF, 5.4 MPa for GF, and 5.1 MPa for PPF.

5. The elastic modulus increased from 38.5 GPa for REF to 43.8 GPa for SF, 41.6 GPa for BF, 40.4 GPa for GF, and 39.2 GPa for PPF, indicating improved stiffness and an enhanced ability of concrete to withstand loads without significant deformation.

6. Fiber reinforcement contributed to reducing the opening width of the major crack under flexural loading. For REF, the crack opening width was 0.95 mm, whereas for SF it decreased to 0.42 mm, for BF to 0.48 mm, for GF to 0.56 mm, and for PPF to 0.61 mm.

7. According to the hydrophysical test results, water absorption decreased by 18.3-29.3%. The minimum water absorption value was obtained for mixture SF at 3.41%, whereas for REF it was 4.82%. For BF, water absorption was 3.56%; for GF, 3.78%; and for PPF, 3.94%.

8. The capillary absorption coefficient decreased from 0.184 kg/(m²·h^0.5) for REF to 0.121 kg/(m²·h^0.5) for SF, 0.129 kg/(m²·h^0.5) for BF, 0.136 kg/(m²·h^0.5) for GF, and 0.148 kg/(m²·h^0.5) for PPF. At the same time, the contact angle increased from 84° for REF to 101° for SF, 98° for BF, 96° for GF, and 95° for PPF.

9. The watertightness grade increased from W10 for the control mixture to W14 for SF and BF, while for GF and PPF it reached W12.

10. Sulfate resistance tests showed a reduction in mass loss from 2.8% for REF to 1.2% for SF, 1.4% for BF, 1.7% for GF, and 1.9% for PPF. The strength retention coefficient increased from 78.7% for REF to 90.3% for SF, 89.4% for BF, 88.9% for GF, and 88.2% for PPF.

11. According to the freeze-thaw resistance test results, mass loss after 300 freeze-thaw cycles decreased from 4.6% for REF to 1.8% for SF, 2.1% for BF, 2.4% for GF, and 2.8% for PPF. The reduction in strength after 300 cycles decreased from 18.4% for REF to 7.6% for SF, 8.9% for BF, 9.8% for GF, and 10.7% for PPF.

12. Based on the combination of physical-mechanical and hydrophysical properties, steel fiber and basalt fiber were identified as the most effective types of dispersed reinforcement.

REFERENCES

1. Ilyassova K.I., Moldamuratov Zh.N., Seitkazinov O.D., Abiyeva G.S., Tukhtamisheva A.Z., Paktin M. Experimental studies of concrete materials for the restoration of hydraulic structures. *Nanotechnologies in construction*. 2025;17(6):697-714. https://doi.org/10.15828/2075-8545-2025-17-6-697-714. – EDN: OBIJOJ.

2. Imanov A.M., Moldamuratov Zh.N., Seitkazinov O.D., Tukhtamisheva A.Z., Ismailova A.B., Rakhimova G.M. Enhanced operational reliability of irrigation canals through the application of modified concrete. *Nanotechnologies in construction*. 2025;17(6):678-696. https://doi.org/10.15828/2075-8545-2025-17-6-678-696. – EDN: MFTDRV.

3. Moldamuratov Zh.N., Imambayeva R.S., Imambaev N.S., Iglikov A.A., Tattibayev S.Zh. Polymer concrete production technology with improved characteristics based on furfural for use in hydraulic engineering construction. *Nanotechnologies in Construction*. 2022;14(4):306-318. https://doi.org/10.15828/2075-8545-2022-14-4-306-318. – EDN: JOZNEX.

4. Mukhopadhyay S., Khatana S. A review on the use of fibers in reinforced cementitious concrete. *Journal of Industrial Textiles*. 2015;45(2):239-264. https://doi.org/10.1177/1528083714529806

5. Yazid M. H., Faris M. A., Abdullah M.M.A.B., Nabiałek M., Rahim S.Z.A., Salleh M.A.A.M., Jeż B. Contribution of Interfacial Bonding towards Geopolymers Properties in Geopolymers Reinforced Fibers: A Review. *Materials*. 2022;15(4). https://doi.org/10.3390/ma15041496

6. Tran N.P., Gunasekara C., Law D.W., Houshyar S., Setunge S. Microstructural characterisation of cementitious composite incorporating polymeric fibre: A comprehensive review. *Construction and Building Materials*. 2022. https://doi.org/10.1016/j.conbuildmat.2022.127497

7. Moldamuratov Zh.N., Iglikov A. A., Sennikov M.N., Madaliyeva E.B., Turalina M.T. Irrigation channel lining using shotcrete with additives. *Nanotechnologies in Construction*. 2022;14(3):227-240. https://doi.org/10.15828/2075-8545-2022-14-3-227-240. – EDN: BIEVUB

ISSN 2075-8545 (online)

8. Rajak M., Rai B. Effect of Micro Polypropylene Fibre on the Performance of Fly Ash-Based Geopolymer Concrete. *Journal of Applied Engineering Sciences*. 2019; 9(1): 97-108. https://doi.org/10.2478/jaes-2019-0013

9. Li Y., Wang Q., Xu S., Song Q. Study of eco-friendly fabricated hydrophobic concrete containing basalt fiber with good durability. *Journal of Building Engineering*. 2023; 65. https://doi.org/10.1016/j.jobe.2022.105759

10. Moldamuratov Z.N., Ussenkulov Z.A., Yeskermessov Z.E., Shanshabayev N. A., Bapanova Z.Z., Nogaibekova M.T., Joldassov S.K. Experimental study of the effect of surfactants and water-cement ratio on abrasion resistance of hydraulic concretes. *Rasayan Journal of Chemistry*. 2023;16(3):1116-1126. https://doi.org/10.31788/RJC.2023.1638391

11. Liu X., Li C., Yu B., Wang H., Feng Y., Pang Y., Wang G. Bond performance between hooked-end steel fibers and hydrophobic fibre reinforced concrete under freeze-thaw cycling. *Construction and Building Materials*. 2025;494. https://doi.org/10.1016/j.conbuildmat.2025.143447

12. Moldamuratov Zh.N., Ismailova A.B., Tukhtamisheva A.Z., Yeskermessov Zh.E., Rakhimov M.A. Experimental study of asphalt concrete as the optimal material for lining irrigation canals. *Nanotechnologies in Construction*. 2024;16(2):125-139. https://doi.org/10.15828/2075-8545-2024-16-2-125-139. – EDN: AROTER.

13. Gamage N., Gunasekara C., Law D.W., Houshyar S., Setunge S., Cwirzen A. Enhancement of concrete performance and sustainability through incorporation of diverse waste carpet fibres. *Construction and Building Materials*. 2024;445. https://doi.org/10.1016/j.conbuildmat.2024.137921

14. Chen Y.X., Yu Q. Surface modification of miscanthus fiber with hydrophobic silica aerogel for high performance bio-lightweight concrete. *Construction and Building Materials*. 2023; 411. https://doi.org/10.1016/j.conbuildmat.2023.134478

15. Barnat-Hunek D., Smarzewski P. Surface free energy of hydrophobic coatings of hybrid-fiber-reinforced high-performance concrete. *Materiali in Tehnologije*. 2015; 49(6): 895-902. https://doi.org/10.17222/mit.2014.174

16. Patel K., Gupta R., Garg M., Wang B., Dave U. Development of FRC materials with recycled glass fibers recovered from industrial GFRP-Acrylic Waste. *Advances in Materials Science and Engineering*. 2019. https://doi.org/10.1155/2019/4149708

17. Ma L., Zhen C., Zeng Q., Li B. Experimental Investigation on the Mechanical Properties of Geopolymer Recycled Aggregate Concrete Reinforced with Steel-Polypropylene Hybrid Fiber. *Buildings*. 2025; 15(10). https://doi.org/10.3390/buildings15101723

18. Malchiodi B., Pelaccia R., Pozzi P., Siligardi C. Three sustainable polypropylene surface treatments for the compatibility optimization of PP fibers and cement matrix in fiber-reinforced concrete. *Ceramics International*. 2023;49(14): 24611-24619. https://doi.org/10.1016/j.ceramint.2023.02.105

19. Muzenski S., Flores-Vivian I., Sobolev K. Durability of superhydrophobic engineered cementitious composites. *Construction and Building Materials*. 2015;81:291-297. https://doi.org/10.1016/j.conbuildmat.2015.02.014

20. Thiyagarajan R., Pazhani K.C. Experimental investigations on the behaviour of PPFRC and SFRC. *International Journal of Advanced Research in Engineering and Technology*. 2019;10(3):194-202. https://doi.org/10.34218/IJARET.10.3.2019.020

21. Kina C., Turk K., Atalay E., Donmez I., Tanyildizi H. Comparison of extreme learning machine and deep learning model in the estimation of the fresh properties of hybrid fiber-reinforced SCC. *Neural Computing and Applications*. 2021;33(18):11641-11659. https://doi.org/10.1007/s00521-021-05836-8

22. Barnat-Hunek D., Smarzewski P. Influence of hydrophobisation on surface free energy of hybrid fiber reinforced ultra-high performance concrete. *Construction and Building Materials*. 2016;102:367-377. https://doi.org/10.1016/j.conbuildmat.2015.11.008

23. Abdouss M., Shokri A., Karimi M.M., Zargaran M. Plasma Oxidation of Polypropylene Fibers for Concrete Reinforcement. *Russian Journal of Applied Chemistry*. 2022;95(3):366-378. https://doi.org/10.1134/S1070427222030053

24. Lu Y., Zhu T., Li S., Liu Z. Bond Behavior of Wet-Bonded Carbon Fiber-Reinforced Polymer-Concrete Interface Subjected to Moisture. *International Journal of Polymer Science*. 2018. https://doi.org/10.1155/2018/3120545

25. Sun Y., Jin Z., Du F., Deng L., Pang B., Yang L., Li S. High performance glass fiber reinforced polymer bars for marine engineering: A synergistic approach using microwave-assisted nanomaterial functionalization and organosilicon modification. *Construction and Building Materials*. 2025;493. https://doi.org/10.1016/j.conbuildmat.2025.143119

26. Corinaldesi V., Moriconi G. Durable fiber reinforced self-compacting concrete. *Cement and Concrete Research*. 2004;34(2):249-254. https://doi.org/10.1016/j.cemconres.2003.07.005

27. Li S., Ye Y., Wu Q., Gao L., Ren H. Preparation of High Performance Hydrophobic Concrete Material and Experimental Study on Its Corrosion Resistance. *Science of Advanced Materials*. 2020;12(9):1341-1351. https://doi.org/10.1166/sam.2020.3825

28. Zhou A., Li K., Yu Z., Yang G., Liu T. Atomic Insight into Durability and Interfacial Stability of Novel Hydrophobic Composite in Concrete Alkaline Environment for Marine Engineering. *Engineering*. 2026. https://doi.org/10.1016/j.eng.2025.12.020

29. Xiong S., Zhang H., Liu W., Zhang L. Resolving the strength-permeability trade-off in recycled aggregate pervious concrete by fiber reinforcement. *Journal of Building Engineering*. 2026; 118. https://doi.org/10.1016/j.jobe.2025.114992

30. Muzenski S., Flores-Vivian I., Sobolev K. Hydrophobic modification of ultra-high-performance fiber-reinforced composites with matrices enhanced by aluminum oxide nano-fibers. *Construction and Building Materials*. 2020;244. https://doi.org/10.1016/j.conbuildmat.2020.118354

31. Sun Y., Jin Z., Yang L. Evolution of Bonding Performance and Improvement Mechanism of Glass Fiber Reinforced Plastics-Concrete Based on Resin Matrix Modification. *Kuei Suan Jen Hsueh Pao/Journal of the Chinese Ceramic Society*. 2024; 52(11):3460-3469. https://doi.org/10.14062/j.issn.0454-5648.20230873

32. Zhakipbayev B.Y., Zhakiyev N.K., Abdikadyr B.Z., Moldamuratov Z.N., Abekov K.O. The Technology of Foam-Glass Building Materials for Heat-Insulating Purposes Using Amorphous-Silica Rocks. *ES Materials and Manufacturing*. 2025; 27. https://doi.org/10.30919/esmm1379

33. Kultayeva S.M., Zhakipbayev B.Y., Moldamuratov Z.N., Kim H.S., Akimbayeva N. Sintering Atmosphere and Polytype Effects on Porous Silicon Carbide Ceramics. *ES Materials and Manufacturing*. 2025;29. https://doi.org/10.30919/mm1757

34. Kultayeva S.M., Zhakipbayev B.Y., Moldamuratov Z.N., Lakhbayeva Z.A. Carbon Nanotubes Effect on The Electrical and Thermal Properties of Porous Silicon Carbide Ceramics. *ES Materials and Manufacturing*. 2025;30. https://doi.org/10.30919/mm1871

35. Bekbasarov I., Nikitenko M., Shanshabayev N., Atenov Y., Moldamuratov, Z. Tapered-prismatic pile: driving energy consumption and bearing capacity. *News of the National Academy of Sciences of the Republic of Kazakhstan, Series of Geology and Technical Sciences*. 2021;6(450):53-63. https://doi.org/10.32014/2021.2518-170X.119

36. Kabdushev A.A., Agzamov F.A., Manapbayev B.Zh., Moldamuratov Zh.N. Microstructural analysis of strain-resistant cement designed for well construction. *Nanotechnology in Construction*. 2023;15(6):564-573. https://doi.org/10.15828/2075-8545-2023-15-6-564-573. – EDN: WFTXGR.

37. Jumadilova S.Zh., Khomyakov V.A., Kenebayeva A.K., Moldamuratov Zh.N. The use of geosynthetic materials to increase the bearing capacity of soil cushions. *Nanotechnologies in Construction*. 2024;16(4):342-354. https://doi.org/10.15828/2075-8545-2024-16-4-342-354. – EDN: KBXJDR.

38. Zhakipbayev B.Ye., Ismailova A.B., Tukhtamisheva A.Z., Seitkazinov O.D., Moldamuratov Zh.N. Energy efficiency and decarbonization of cement and foamed glass production through the use of natural active mineral additives (opoka and diatomite). *Nanotechnologies in Construction*. 2024;16(6):587-600. https://doi.org/10.15828/2075-8545-2024-16-6-587-600. – EDN: RUQCWE.

39. Rakhimov M.A., Aubakirova Z.A., Aldungarova A.K., Menéndez Pidal de Navascués I., Moldamuratov Zh.N. Optimization of a sustainable composition of fine-grained concrete for 3D printing with partial substitution of sand with fly ash and slag waste. *Nanotechnologies in Construction*. 2025;17(3):296-306. https://doi.org/10.15828/2075-8545-2025-17-3-296-306. – EDN: BISWAS.

ADDITIONAL INFORMATION

During the preparation of this article, the artificial intelligence tool ChatGPT 5.2 was used exclusively for checking the text for grammatical, spelling, and stylistic errors, as well as, in some cases, for improving wording and text structure. The content and scientific substance of the article were prepared entirely by the authors and are not the result of generative text creation. After using the ChatGPT 5.2 artificial intelligence tool, the text was additionally reviewed, edited, and revised by the authors as necessary. The authors bear full responsibility for the content of the published article.

INFORMATION ABOUT THE AUTHORS

Manizha Paktin – Master's degree, Assistant Professor, School of Construction, International Educational Corporation, 050043, Almaty, 28 K. Ryskulbekov Street, Kazakhstan, m.paktin@kazgasa.kz, https://orcid.org/0009-0006-7348-2372

Alibek M. Imanov – PhD doctoral student, Abylkas Saginov Karaganda Technical University, 100027, Karaganda, 56 N. Nazarbayev Avenue, Kazakhstan, alibek.imanov@mail.ru, https://orcid.org/0009-0006-6579-8510

Karlygash I. Ilyassova – Master's degree, Assistant Professor, School of Engineering, International Educational Corporation, 050043, Almaty, 28 K. Ryskulbekov Street, k.iliasova@kazgasa.kz, https://orcid.org/0000-0002-6994-4806

Orazaly D. Seitkazinov – Cand. Sci. (Eng.), Professor, School of Construction, International Educational Corporation, 050043, Almaty, 28 K. Ryskulbekov Street, Kazakhstan; 050043, Almaty, 29 Toraigyrov Street, Kazakhstan, oseitkazinov@mail.ru, https://orcid.org/0000-0002-4854-3747

Manat T. Nogaibekova – Senior Lecturer, School of Architecture and Logistics, Kazakh National University of Water Management and Irrigation, 080003, Taraz, 28 Satpayev Street, Kazakhstan, nogaibekova_m@mail.ru, https://orcid.org/0000-0002-4394-4453

Zhangazy N. Moldamuratov – PhD, Research Professor, School of Construction, International Educational Corporation, 050043, Almaty, 28 K. Ryskulbekov Street, Kazakhstan; 050043, Almaty, 29 Toraigyrov Street, Kazakhstan, zhanga_m_n@mail.ru, https://orcid.org/0000-0002-4573-1179

CONTRIBUTIONS OF THE AUTHORS

M. Paktin – conducted the main part of the experimental research, prepared and manufactured the specimens, performed tests on strength, water absorption, freeze-thaw resistance, and sulfate resistance, processed the experimental data, prepared the initial version of the manuscript, and organized the presentation of the research results.

A.M. Imanov – participated in the development of research methodology and the selection of concrete mixtures, analyzed the physical-mechanical and hydrophysical characteristics, interpreted the results related to strength, crack resistance, watertightness, and durability, prepared individual sections of the article, and participated in the discussion of the results.

K.I. Ilyassova – carried out microstructural investigations, interpreted the data on the phase composition and microstructure of the cement matrix, prepared figures, diagrams, and descriptions of the microstructural features of the investigated mixtures, and participated in writing and editing the article.

O.D. Seitkazinov – participated in laboratory testing, specimen preparation and storage, processing of selected experimental results, and discussion of the obtained data.

M.T. Nogaibekova – participated in the analysis of scientific literature, selection and systematization of bibliographic sources, preparation of tables, figures, and reference list, as well as in the technical preparation of the manuscript for publication.

Zh.N. Moldamuratov – provided scientific supervision of the study, developed the overall concept and structure of the article, formulated the research aim and objectives, coordinated the implementation of the experimental program, analyzed and generalized the obtained results, prepared the conclusions and final remarks, performed scientific editing, and approved the final version of the manuscript for publication.

The authors declare no conflicts of interests.

The article was submitted 07.04.2026; approved after reviewing 03.06.2026; accepted for publication 10.06.2026.